MEASUREMENT OF ACOUSTIC IMPEDANCE OF THE HUMAN EAR

By

TUSHAR SHANKAR KALE

Bachelor of Engineering
Nagpur University
Nagpur, India
1972

Master of Engineering
Indian Institute of Science
Bangalore, India
1974

Submitted to the Faculty of the Graduate College
of the Oklahoma State University
in partial fulfillment of the requirements
for the Degree of
DOCTOR OF PHILOSOPHY
December, 1979

MEASUREMENT OF ACOUSTIC IMPEDANCE OF THE HUMAN EAR

Thesis Approved:

Larry D. Tokle
Thesis Adviser

Karen M. Reed

Richard L. Lowery

Ronald O. Rhoten

Norman N. Durham
Dean of the Graduate College

ACKNOWLEDGMENTS

Many individuals who in some way contributed to this work cannot be recognized in these brief acknowledgments. However, the author does wish to express his appreciation to those most directly involved.

I wish to express my sincere appreciation and thanks to my thesis adviser, Dr. Larry D. Zirkle, for his cooperation and excellent guidance. His confidence in my ability and personal counsel throughout the course of this graduate study are gratefully acknowledged.

My special thanks to Dr. Richard L. Lowery for his guidance and assistance during this work. His confidence and unselfish interest in my success have been an example which I can only hope to follow. I wish to thank Dr. Karl N. Reid for his interest as expressed by the time he spent with me discussing the thesis work. I would like to thank Dr. Ronald P. Rhoten for serving on my advisory committee and for his interest and assistance during this work.

I thank the School of Mechanical and Aerospace Engineering of the Oklahoma State University for providing me with financial assistance during the course of my study.

I wish to thank Mrs. Grayce Wynd for typing the final draft of this thesis.

I am particularly indebted to my parents, whose spiritual, material, and inspirational encouragement and thorough understanding have made this goal possible.

TABLE OF CONTENTS

TABLE

LIST OF FIGURES

LIST OF SYMBOLS

A_i, B_i, C_i, D_i	- four-pole matrix elements of a segment
A_{Pi}, B_{Pi}, C_{Pi}, D_{Pi}	- four-pole matrix elements of a probe tube
C	- velocity of sound (cm/sec)
P_i	- pressure at section 1 (dynes/cm^2)
P_2	- pressure at section 2 (dynes/cm^2)
P_U	- pressure at the unknown impedance (dynes/cm^2)
P_{1m}	- pressure measured by input microphone (dynes/cm^2)
P_{2m}	- pressure measured by output microphone (dynes/cm^2)
U_1	- volume velocity at section 1 (cm^3/sec)
U_2	- volume velocity at section 2 (cm^3/sec)
U_U	- volume velocity at unknown impedance (cm^3/sec)
U_{1m}	- volume velocity at input microphone (cm^3/sec)
U_{2m}	- volume velocity at output microphone (cm^3/sec)
U_P	- volume velocity input to the probe tube (cm^3/sec)
U_{in}	- volume velocity input to section 2 (cm^3/sec)
Z_2	- acoustic impedance at section 2 (dyne-sec/cm^5)
Z_3	- acoustic impedance at section 3 (dyne-sec/cm^5)
Z_c	- characteristics impedance of a tube (dyne-sec/cm^5)
Z_e	- impedance at the ear drum (dyne-sec/cm^5)
Z_K	- known impedance (dyne-sec/cm^5)
Z_P	- input impedance of probe tube (dyne-sec/cm^5)
Z_S	- standard impedance (dyne-sec/cm^5)

Z_{CV} - impedance of the cavity (dyne-sec/cm^5)

Z_{in} - input impedance of segment 2 (dyne-sec/cm^5)

Z_{mic} - input impedance of a microphone (dyne-sec/cm^5)

J_o - Bessel function of first kind of order zero

J_1 - Bessel function of first kind of order one

L_1 - length of segment 1 (cm)

L_2 - length of segment 2 (cm)

L_e - equivalent length of a tube (cm)

R - radius of a tube (cm)

R' - pressure ratio

α - attenuation constant

β - phase constant

ν - ratio of specific heats of air

ρ - density of air (gm/cm^3)

σ - Prandtl number of air

τ - complex propagation operator (1/cm)

μ - absolute viscocity of air (gm/sec-cm)

ω - radian frequency (rad/sec)

CHAPTER I

INTRODUCTION

1.1 Acoustic Impedance of the Human Ear

Although the concept of acoustic impedance was introduced by Webster (1) in 1914, its application to clinical audiology did not become evident until Metz (2) published his classic monograph entitled "The Acoustic Impedance Measurement on Normal and Pathological Ears." Since then, numerous investigators have studied acoustic impedance and its relationship to the pathological condition of a human ear and voluminous amounts of literature have accumulated on the subject. It is now a well established fact that impedance measurement provides more information about the condition of an ear than any other external (in vitro) source of information such as case history, audiometry, or otoscopic examination.

The audiometric examinations provide only indirect and nonspecific information about the state of the middle ear. They are directed primarily toward differentiating middle ear disorder from sensori neural impairment. No differentiation among the middle ear malfunction can be made solely on the basis of audiometric tests. The otoscopic examination, on the other hand, is limited to directly visible anatomical changes and to a qualitative evaluation of the ear drum mobility at amplitudes that far exceed the normal physiological range. The examination gives inconclusive results in all cases of conductive hearing

loss except those that are associated with gross changes of ear drum anatomy, position or mobility. With respect to the middle ear disorder, the diagnostic information from acoustic impedance measurement goes considerably beyond that which can be derived from otoscopic examination and audiometric tests.

1.2 Static Impedance Profiles

Current clinical methods using impedance measurement may be divided into three categories: (a) Measurement of Static Impedance (absolute impedance); (b) Measurement of Dynamic Impedance, and (c) Tympanometry.

Static acoustic impedance measurements are made with atmospheric air pressure in the ear canal and with the middle ear muscles in the state of normal condition. These measurements reflect directly the transmission characteristics of the middle ear system and are of primary value in differential diagnosis of conducting hearing loss. In general, acoustic impedance at the ear drum is (a) lower than normal for discontinuity of the ossicular chain; (b) higher than normal for clinical otosclerosis, and (c) very much higher than normal with chronic disease of the middle ear.

In a normal ear, contraction of middle ear muscles produces a measurable change in acoustic impedance at the ear drum. The change in impedance is termed as a dynamic impedance. The normal relation between changes in acoustic impedance and reflexive contractions of the middle ear muscles is modified by the middle ear disease. These measurements are used mainly for detecting conductive hearing impairment.

Acoustic impedance at the ear drum of a normal ear changes if air pressure in the ear canal is made higher or lower than the ambient air

pressure. This predictable relationship between changes in air pressure and changes in acoustic impedance is modified by middle ear disease, by perforations of the ear drum, by abnormal air pressure in the middle ear or by scars on the ear drum. The general term "Tympanometry" refers to methods and techniques for measuring and evaluating changes in acoustic impedance with systematic changes in air pressure.

In addition to the three categories of clinical methods described above, in recent years a fourth category is receiving attention. It is measurement of static acoustic impedance at various frequencies (3).

If the static impedance of an ear is measured at several frequencies, the resulting plot of impedance versus frequency is called an impedance profile. It is possible that such an impedance profile contains additional information about the pathological condition of the middle ear. In spite of its clinical application, this concept was not studied thoroughly earlier, mainly because of lack of suitable instruments to measure the static impedance of the human ear over a wide frequency range. A systematic investigation of the possibility of diagnostic information in static impedance profile was done by Whaley (3). He showed impedance profiles associated with middle ear pathology to be distinctly different from normal impedance profiles. However, his investigation was restricted to frequencies below 1000 Hz. He observed that for certain pathological conditions, peaks occurred in the middle ear profiles. As significant hearing occurs at high frequencies, it is desirable to be able to measure acoustic impedance over an extended frequency range. Design and development of an instrument that would measure the acoustic impedance of a human ear over a wide frequency range is the subject of this dissertation. Such an instrument would be

of great value in auditory research, and perhaps eventually as a diagnostic tool in clinical audiology.

1.3 Instrumentation

Several methods of measuring acoustic impedance of material are described by Beranek (4). However, most of these methods cannot be adopted for measuring impedance of a human ear mainly because of the heavy and bulky instrumentation employed in the measurement process. Among the methods currently in use for ear impedance measurement, most are based on the assumption that volume velocity of a sound source is constant (5-8). If the volume velocity of the source is known, then measured sound pressure is directly proportional to the acoustic impedance of the medium. A major limitation of this technique is that it introduces error in phase measurement. Secondly, the assumption of constant volume velocity depends on a large source impedance. The value of internal source impedance of acoustical devices is difficult to check. Thus, the validity of the assumption of constant volume velocity is questionable in most cases. The advantage of the method is that it is simple and no complex modeling of acoustic elements of the measuring device is needed. In the present investigation, experiments are conducted to check the validity of the constant volume velocity assumption.

Another method that has received much attention in the past is an acoustic bridge technique (9). Similar to the bridge technique in electrical engineering, an unknown impedance is determined by comparing it with the known acoustical impedances. The main requirement of this technique is the availability of stable, accurately calibrated standards

of inductance, capacitance and resistance, at least one of which is continuously variable. Although adequate standards have been developed for electrical measurements, suitable standards of acoustical resistance, mass and compliance have not been available. Moreover, at high frequencies, the characteristics of the acoustical elements change. For example, a cavity that behaves as a pure compliance at low frequency will have resistance and inertance at high frequencies.

For investigating the diagnostic value of impedance profiles, Whaley (3) developed an impedance meter based on a technique that requires measurement of pressures at two points on a tube having a sound source at one end and an unknown impedance at the other end. He used a lumped parameter approach to obtain the equivalent acoustic circuit of his instrument. Then, applying Thevenin's theorem to the acoustic circuit and using two pressure measurements, he obtained internal source impedance and open circuit pressure of the sound source. He thus calibrated the sound source and then used it to measure the unknown impedance. Since the theory of the instrument is based on lumped parameter models, working of the instrument is limited to low frequency (up to 1000 Hz). The frequency range may be improved by reducing the dimensions of the instrument, but there is a practical limit below which the pressure measurements are extremely difficult. The instrument described in the following chapters is based on a technique that is applicable at high frequencies and does not require any assumption about the volume velocity of the sound source. A brief account of the technique is given in the following section.

1.4 Methodology

The acoustic impedance of a material is defined as a complex ratio of pressure to volume velocity normal to the surface of the material. The main problem associated with impedance measurement is that volume velocity cannot be measured directly. In the measurment technique described in this dissertation, volume velocity is measured by indirect means. This is achieved by measuring pressures at any two sections on a tube connected to an unknown impedance, and using a mathematical model of the tube. The mathematical model is essentially a relationship between four variables, namely, pressures and volume velocities at any two sections on the tube, in the form of two independent equations. Thus, knowing two pressures, volume velocities can be calculated using the mathematical model. The acoustic impedance at any of the two sections, for example, is then obtained by taking the ratio of measured pressure and calculated volume velocity at that section. Once the impedance at any section of the tube is known, it can be related to impedance at any other section by employing the same mathematical model.

In this method of impedance measurement, the accuracy of measured impedance depends, among other things, on the accuracy of the mathematical model representing the tube. Various papers have been published on the subject of modeling of a tube, often in relation to the studies dealing with dynamic response of pressure transmission lines (10-13). As a result, different models of varying complexity are available in the literature. Among these, the distributed parameter model, as derived by Iberall (10), is used in the present study. It is the most accurate and is valid over the frequency range of interest in the present study. The accuracy of measurement is then checked by

measuring standard impedances. The instrument is then employed to measure the acoustic impedance of a normal human ear. The instrument measures the impedance at the tip of the ear canal. In order to obtain the impedance at the ear drum, the effect of the ear canal must be taken into account. In previous studies, the ear canal was assumed as a shunt compliance. This is a reasonable assumption only at low frequency. In the present study, the ear canal is represented by a distributed parameter model and the impedance profile up to 7 kHz for a normal human ear is obtained.

1.5 Organization

The dissertation is presented in the following format: Chapter II introduces the basic working principles of the instrument. The mathematical model of the tube is presented, and experiments validating the model are described. Based on the principles described in Chapter II, the measuring instrument is designed. Chapter III contains the design procedure and details of the instrument. Experiments to check the measurement accuracy of the instrument are described. The instrument is then employed to measure the acoustic impedance of a normal human ear. The measurement procedure and the impedance profile of a normal human ear are presented in Chapter IV. Finally, Chapter V presents the conclusions and indicates areas of future research.

CHAPTER II

THE IMPEDANCE MEASUREMENT TECHNIQUE

2.1 Introduction

The need to develop an instrument to measure the acoustic impedance of a human ear was established in the last chapter. As previously noted, it is required to operate over a wide frequency range. Presently, available instruments are either based on the principles that are valid only for low frequencies, or are based on some assumptions (e.g., assuming the volume velocity of the sound source to be constant) whose validity is difficult to check. In this chapter, a technique that is free from the above limitations to measure the acoustic impedance is described.

2.2 Principle of Measurement

Consider a cylindrical tube with an unknown impedance at one end and excited by a sound source connected to its other end as shown in Figure 1. It is required to measure the unknown impedance at the end of the tube.

Let P_u and U_u represent pressure and volume velocity at the load end. These are related to the unknown impedance Z_u by the following equation:

$$P_u/U_u = Z_u \tag{2.1}$$

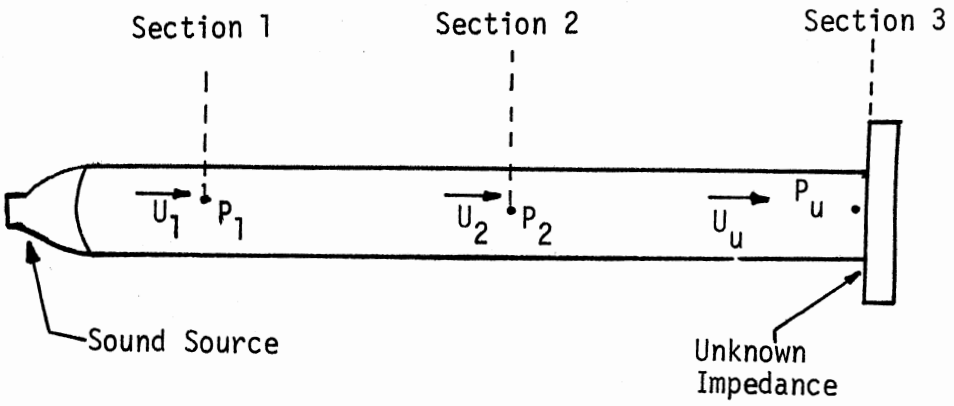

Figure 1. A Typical Acoustic System

Since it is not possible with the conventional technology to measure volume velocity, Equation (2.1) cannot be employed directly to evaluate the unknown impedance. In the measurement technique described below, the impedance is obtained by measuring pressures at two points on the tube and using a mathematical model of the tube.

Referring to Figure 1, let P_1, U_1, and P_2, U_2 be the pressures and volume velocities at any two sections on the tube. The mathematical model is a relationship in the form of two independent equations between these four variables. If two pressures are measured, volume velocities can be computed by using these equations. The impedance, Z_2, at section two is then obtained by taking a ratio of measured pressure, P_2, and the calculated volume velocity, U_2. Once the impedance at section two is obtained, the unknown impedance can be evaluated by applying the mathematical model to the portion of the tube between section two and section three. Derivation of the mathematical model of a tube is presented below.

2.2.1 Modeling of a Tube

Consider a cylindrical tube shown in Figure 2. A mathematical relation describing the sound pressure and volume velocity at the entrance to the tube (section 1) in terms of the sound pressure and volume velocity at the exit of the tube (section 2) is desired. With reference to Figure 2, the incident and reflected waves of pressure and volume velocity are described by

$$P_i\ (x,t) = A_i * \text{Exp}\ (j\omega t - \tau x) \qquad (2.2)$$

$$P_r\ (x,t) = A_r * \text{Exp}\ (j\omega t + \tau x) \qquad (2.3)$$

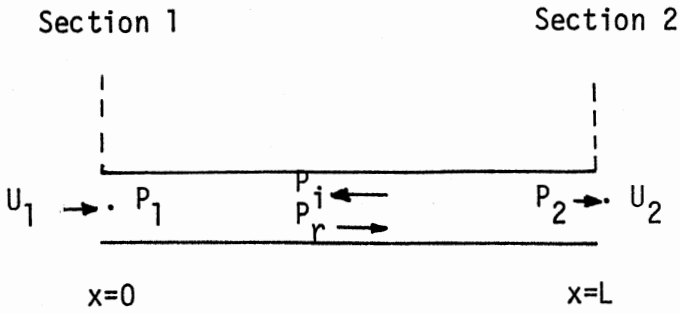

Figure 2. Sound Transmission Through Right Circular Cylindrical Tube

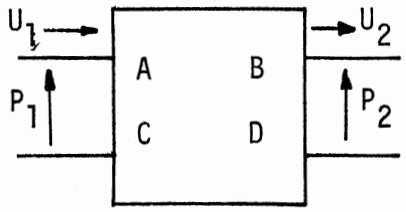

Figure 3. Electrical Analog Four-pole Network Model of the Tube in Figure 2

$$U_i(x,t) = (A_i/Z_c) * \text{Exp}(j\omega t - \tau x) \quad (2.4)$$

$$U_r(x,t) = -(A_r/Z_c) * \text{Exp}(j\omega t + \tau x) \quad (2.5)$$

where

$P_i(x,t)$, $P_r(x,t)$ = sound pressure of incident and reflected waves respectively as a function of distance x and time t

$U_i(x,t)$, $U_r(x,t)$ = volume velocity of incident and reflected waves respectively as a function of distance x and time t

A_i and A_r = complex amplitude coefficient for incident and reflected sound pressure waves respectively

$\tau = \alpha + j\beta$ = complex propagation operator where α represents tube attenuation and β represents the phase constant

Z_c = characteristic impedance of the tube

x = distance along the axis of the tube

t = time, and

$j = \sqrt{-1}$

The total pressure and volume velocity at any section on the tube is obtained by summing the incident and reflected waves of pressure and volume velocity.

$$P(x,t) = A_i \text{Exp}(j\omega t - \tau x) + A_r \text{Exp}(j\omega t + \tau x) \quad (2.6)$$

$$U(x,t) = (A_i \text{Exp}(j\omega t - \tau x) - A_r \text{Exp}(j\omega t + \tau x))/Z_c \quad (2.7)$$

Let the boundary conditions be defined as follows. At section 1,

$$x = 0,\ P(0,t) = P_1\ \text{Exp}\ (j\omega t),\ U(0,t) = U_1\ \text{Exp}\ (j\omega t)$$

and at section 2,

$$x = L_1,\ P(L_1,t) = P_2\ \text{Exp}\ (j\omega t),\ U(L_1,t) = U_2\ \text{Exp}\ (j\omega t)$$

Substituting these boundary conditions in Equations (2.6) and (2.7), the result is

$$P_1 = A_i + A_r \tag{2.8}$$

$$Z_c * U_1 = A_i - A_r \tag{2.9}$$

and

$$P_2 = A_i * \text{Exp}\ (-\tau L_1) + A_r * \text{Exp}\ (\tau L_1) \tag{2.10}$$

$$Z_c * U_2 = A_i * \text{Exp}\ (-\tau L_1) - A_r * \text{Exp}\ (\tau L_1) \tag{2.11}$$

Solving for A_i and A_r from Equations (2.8) and (2.9), the result is

$$A_i = (P_1 + Z_c * U_1)/2 \tag{2.12}$$

$$A_r = (P_1 - Z_c * U_1)/2 \tag{2.13}$$

Substituting Equations (2.12) and (2.13) in Equations (2.10) and (2.11), and solving for P_2 and U_1 and using the definition of hyperbolic functions, the result is

$$P_1 = \text{Cosh}\tau L_1 * P_2 + Z_c * \text{Sinh}\tau L_1 * U_2 \tag{2.14}$$

$$U_1 = (\text{Sinh}\tau L_1/Z_c) * P_2 + \text{Cosh}\tau L_1 * U_2 \tag{2.15}$$

Now, rewriting Equations (2.13) and (2.14) in matrix notation, the result is

$$\begin{bmatrix} P_1 \\ U_1 \end{bmatrix} = \begin{bmatrix} A & B \\ C & D \end{bmatrix} \begin{bmatrix} P_2 \\ U_2 \end{bmatrix} \tag{2.16}$$

where $\begin{bmatrix} A & B \\ C & D \end{bmatrix}$ is the matrix of four-pole parameters of the tube which are defined as follows:

$$\begin{aligned} A &= \text{Cosh}\tau L_1 \\ B &= Z\ \text{Sinh}\tau L_1 \\ C &= \text{Sinh}\tau L_1 / Z_c \\ D &= \text{Cosh}\tau L_1 \end{aligned} \tag{2.17}$$

Equation (2.16) is now in a classical format which is characteristic of a four-pole network. Figure 3 shows the four-pole electric analog of the cylindrical tube carrying sound waves shown in Figure 2, where A, B, C, and D terms represent the classical four-pole parameters, as defined by Equation (2.17). Such representation of an acoustic element is very useful in analyzing a complex acoustic system. Acoustic transmission tubes connected in series are analyzed by using analogous series connected four-pole electric network and parallel-connected tubes are evaluated as parallel connections of four-pole networks.

2.2.2 Measurement of Acoustic Impedance

The mathematical model of the tube discussed above is now applied to the acoustic system shown in Figure 1 to obtain the unknown impedance. The acoustic system is shown in Figure 4(a) with the tube divided into two segments of length, L_1 and L_2. A four-pole network model of the two

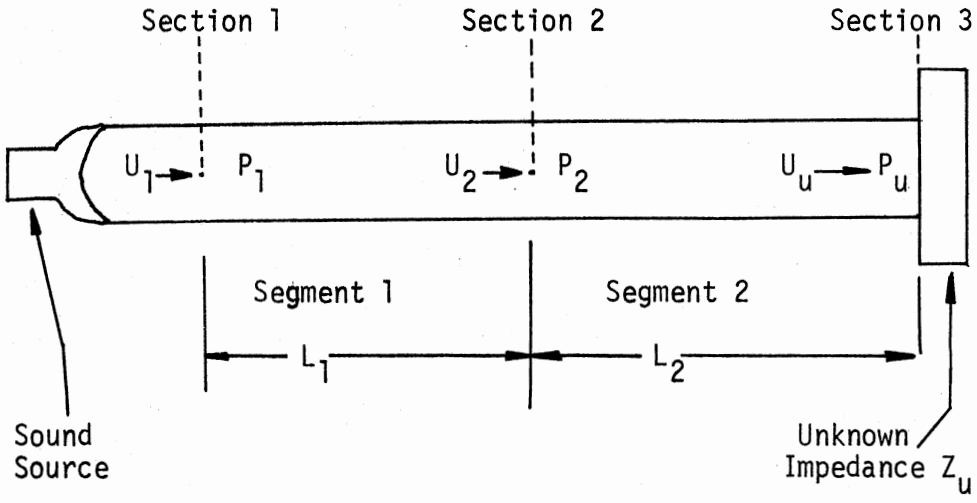

a) Acoustic System

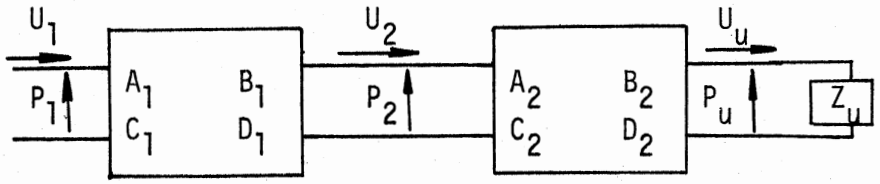

b) Four-pole Network Analog of the Acoustic System

Figure 4. Illustration of Acoustic Impedance Measurement Principle

segments is shown in Figure 4(b). These models are assumed to be completely specified. Let pressures P_1 and P_2 at the ends of segment 1 be measured. The network equation for this segment can be written as

$$P_1 = A_1 * P_2 + B_1 * U_2 \tag{2.18}$$

If Z_2 represents the impedance at section 2, then at that section

$$P_2 = Z_2 * U_2 \tag{2.19}$$

Solving Equation (2.19) for U_2 and substituting it in Equation (2.18), the result is

$$P_1 = (A_1 + B_1/Z_2) * P_2$$

or

$$Z_2 = B_1/(R' - A_1) \tag{2.20}$$

where

$$R' = P_1/P_2 \tag{2.21}$$

The network equations for segment 2 can be written as

$$P_2 = A_2 * P_u + B_2 * U_u \tag{2.22}$$

$$U_2 = C_2 * P_u + D_2 * U_u \tag{2.23}$$

Also at section 3

$$P_u/U_u = Z_u \tag{2.24}$$

Dividing Equation (2.22) by Equation (2.23), and using Equations (2.19) and (2.24), the result is

$$Z_2 = (A_2 * Z_u + B_2)/(C_2 * Z_u + D_2)$$

or

$$Z_u = (B_2 - D_2 * Z_2)/(C_2 * Z_2 - A_2) \qquad (2.25)$$

Equations (2.20) and (2.25) are the desired relations which indicate that the unknown impedance connected to the end of the tube can be obtained by measuring pressures at two points on the tube and using the tube parameters τ and Z_c.

The method described above does not impose any restriction on the properties of sound source (such as high internal source impedance, etc.). Hence, any sound source generating pure tone can be employed for impedance measurement.

While deriving Equations (2.20) and (2.25), the two pressures are assumed to be known. In fact, they must be measured by a microphone or a probe tube with a microphone, and the presence of any of these elements affects the sound field inside the tube. Hence, the above equations need to be modified to take into account this effect. The modified equations are described in the next chapter.

2.3 Tube Parameters

The measurement technique described above employs the tube parameters τ and Z_c in the computation of the unknown impedance. Accurate measurement of the impedance, therefore, requires precise values of

these parameters. The exact equations for τ and Z_c are derived by Iberall (10). Starting with the basic equations of Navier-Stokes, the energy equation, equation of state and continuity, he obtained a simplified set of equations assuming that

(a) fluid medium in the tube is continuous

(b) fluid medium in the tube is excited by small amplitude perturbations

(c) tube wall is rigid

(d) tube wall is isothermal

(e) tube is long enough so that end effects are negligible

(f) fluid medium in the tube is such that $\mu/\rho cR << 1$

(g) excitation frequency, ω, is such that $\mu\omega/\rho c^2 << 1$ and $\omega R/c << 1$

(h) acoustic pressure is uniform over the tube crossection (i.e., plane wave of pressure).

The simplified equations are then solved to obtain the equations for τ and Z_c. The results are:

$$\tau = j\frac{\omega}{c}\left[\frac{1+2(\nu-1)\left[J_1(\alpha' R)/\alpha R J_0(\alpha' R)\right]}{1-2J_1(\beta' R)/\beta' R J_0(\beta' R)}\right] \tag{2.26}$$

and

$$Z_c = \frac{\rho c}{\pi R^2}\left(\left[1 - \frac{2J_1(\beta' R)}{\beta R J_0(\beta R)}\right]\left[1+2(\nu-1)\frac{J_1(\alpha' R)}{\alpha R J_0(\alpha R)}\right]\right)^{-\frac{1}{2}} \tag{2.27}$$

where

$$\alpha' = (- j\omega\rho\sigma/\mu)^{\frac{1}{2}}$$

$$\beta' = (- j\omega\rho/\mu)^{\frac{1}{2}}$$

Before using these equations in the development of the measuring technique, an experiment is performed to check their validity. In the experiment described below, a mathematical model of a tube is created by representing it as a four-pole element. Using the values of τ and Z_c as given by Equations (2.26) and (2.27) in the modeling equations of the tube, the theoretical ratio of input and output pressures of the tube is calculated. This ratio is then compared against the experimentally observed pressure ratio.

A schematic diagram of the experimental setup is shown in Figure 5. A tube used in the experiment is 3 cm long and has an inside diameter of 0.32 cm. This tube is selected because it is used later as a probe tube of the instrument to measure pressure in the impedance tube.

The tube is connected to a 1/2-inch B&K microphone through a specially constructed spacer. The spacer provides a finite distance between the tube and the microphone diaphragm over which the acoustical waves emanating from the tube outlet can regain their plane configuration before striking the diaphragm. If the tube is attached directly to the microphone, the waves do not have sufficient space to regain their plane configuration before striking the diaphragm and the requirement for plane waves of pressure, given as a requirement above, is violated.

The tube-microphone assembly under investigation is connected to one end of a long waveguide, and the latter is excited by a sound source connected to its other end. The use of the long waveguide ensures that

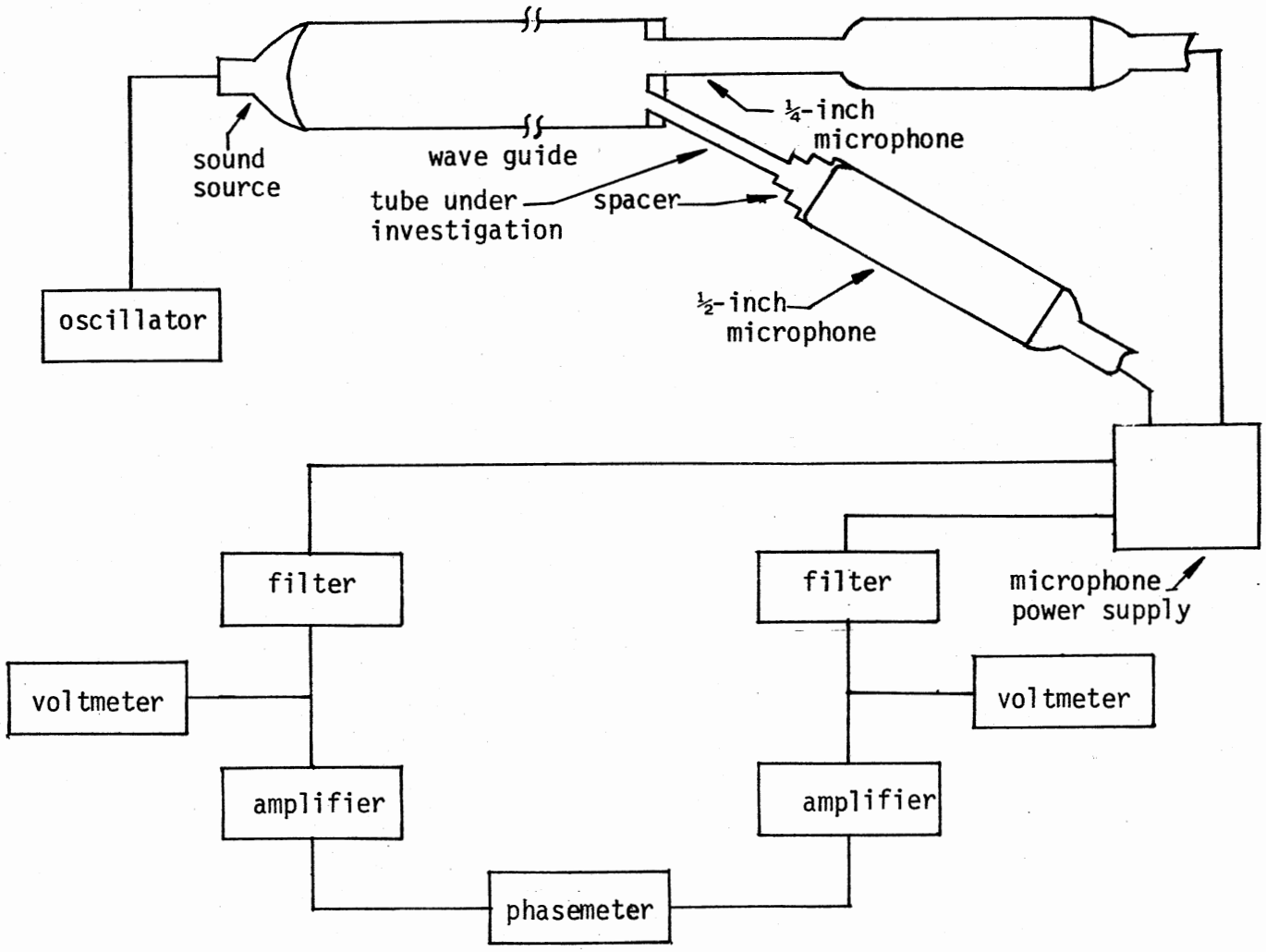

Figure 5. Experimental Setup to Validate the Mathematical Model

pressure waves reaching the tube have gained stable configuration. Input pressure to the tube is measured by installing a ¼-inch B&K microphone so that the microphone diphragm is in flush with the input end of the tube. The ½-inch microphone measures the pressure at the output end of the tube-spacer assembly.

The output voltages of both the microphones are filtered by identical high pass R-C filters, and measured by digital voltmeters. Phase angle between the voltages is measured by the B&K digital phase angle meter.

A schematic diagram of the tube with a spacer and its analog four-pole network model is shown in Figure 6. The subscripts on the four-pole parameters in Figure 6(b) identify their association with the numbered cylindrical tubes given in Figure 6(a). The quantity Z_{mic} represents the impedance of the ½-inch microphone. The real and imaginary parts of Z_{mic} are presented in Figure 7. The microphone impedance data presented in this figure are calculated from the data provided in the manufacturer's handbook.

In Figure 6(c), the circuit of Figure 6(b) has been reduced to a single equivalent four-pole block. The elements of this block are obtained by simple matrix multiplication:

$$\begin{bmatrix} A_{P1} & B_{P1} \\ C_{P1} & D_{P1} \end{bmatrix} = \begin{bmatrix} A_1 & B_1 \\ C_1 & D_1 \end{bmatrix} \begin{bmatrix} A_2 & B_2 \\ C_2 & D_2 \end{bmatrix} \begin{bmatrix} A_3 & B_3 \\ C_3 & D_3 \end{bmatrix} \begin{bmatrix} A_4 & B_4 \\ C_4 & D_4 \end{bmatrix}$$

The circuit equations for the circuit of Figure 6(c) are:

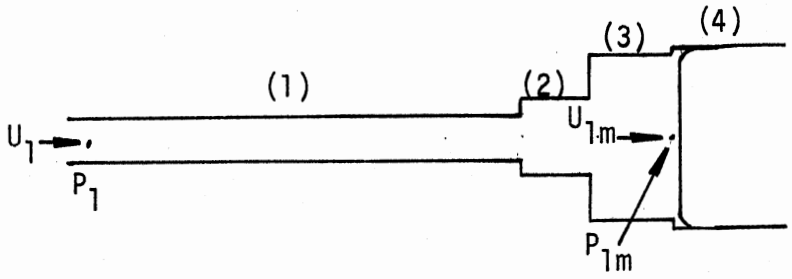

(a) Probe Tube and Spacer

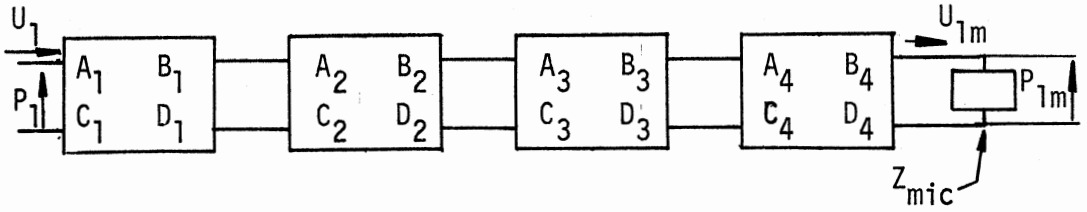

(b) Four-pole Network Analog

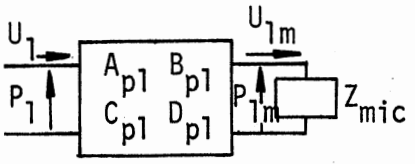

(c) Equivalent Four-pole Network

Figure 6. Probe Tube With Spacer and Its Equivalent Four-pole Model

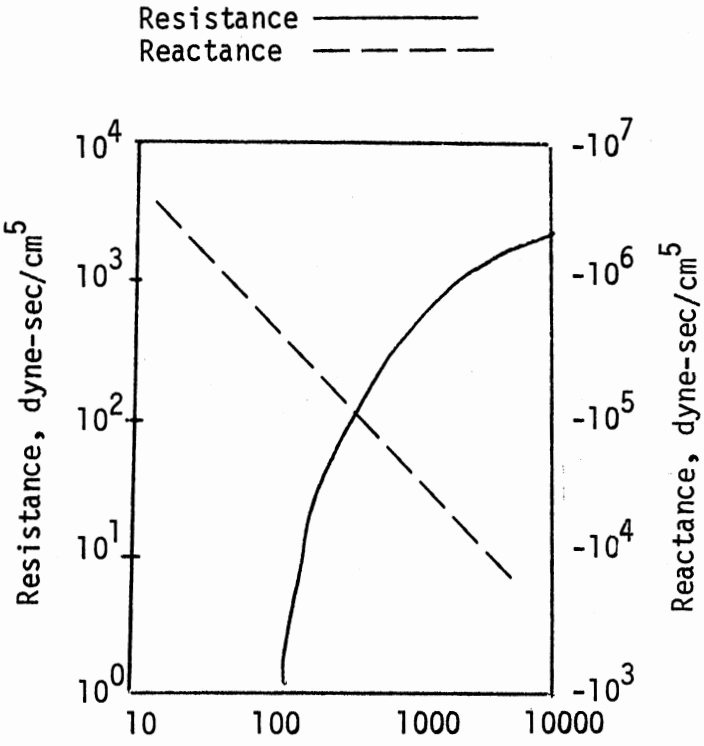

Figure 7. Acoustic Impedance of ½-inch B&K Microphone

$$P_1 = A_{P1} * P_{1m} + B_{P1} * U_{1m} \tag{2.28}$$

$$U_1 = C_{P1} * P_{1m} + D_{P1} * U_{1m} \tag{2.29}$$

$$P_{1m} = Z_{mic} * U_{1m} \tag{2.30}$$

where

P_1, P_{1m} = complex amplitude of pressure at the input end of the tube and at the microphone diaphragm, respectively (dyne/cm^2)

U_1, U_{1m} = complex amplitude of volume velocity at the input end of the tube and at the microphone diaphragm (cm^3/sec), respectively

Solving Equation (2.30) for U_{1m} and substituting in Equation (2.28) and simplifying, the result is

$$P_1/P_{1m} = A_{P1} + B_{P1}/Z_{mic} \tag{2.31}$$

Equation (2.31) gives the theoretical ratio of input and output pressures of the tube.

The experimental pressure ratio can be obtained by referring to Figure 8, which shows the block diagram representation of the experimental setup shown in Figure 5. The quantities appearing in the figure are defined below.

S = sensitivity of the microphone (mv/dynes/cm^2)

ϕ = phase lag of voltage output behind the pressure input to the microphone (degrees)

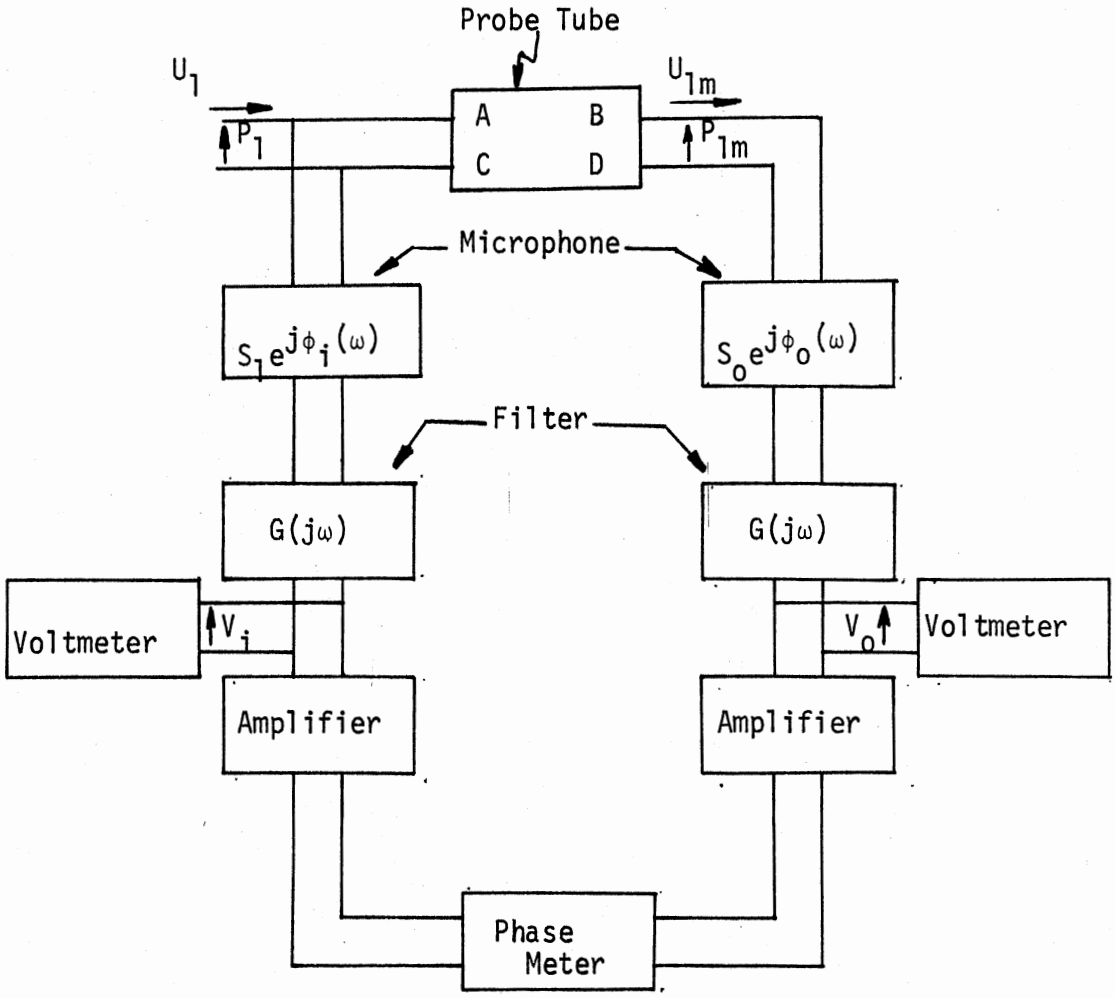

Figure 8. Block Diagram of the Experimental Setup

$G(j\omega)$ = gain of the filter

i, o = subscripts representing input and output side of the tube

ω = radial frequency (radians/sec)

With the above definitions, P_1 and P_{1m} are related to measured voltages V_i and V_o as follows:

$$V_i = P_1 * G(j\omega) * S_i * \text{Exp}\ (j\phi_i(\omega))$$

$$V_o = P_{1m} * G(j\omega) * S_o * \text{Exp}\ (j\phi_o(\rho)) * \text{Exp}\ (j\phi(\omega))$$

The pressure ratio is then given by

$$P_1/P_{1m} = \frac{V_i}{V_o}\ \frac{S_o}{S_i}\ e^{j(\phi_o(\omega) - \phi_i(\omega) + \phi(\omega))} \qquad (2.32)$$

where ϕ is the phase angle of V_o with respect to V_i measured by the phase angle meter. The quantity $\phi_i(\omega)$ and $\phi_o(\omega)$ for the ¼-inch and ½-inch microphones are obtained from the manufacturer's handbook and are presented in Figure 9. Thus, measuring two voltages and the phase angle between them, the experimental pressure ratio is calculated using Equation (2.32).

The experiment was conducted from 150 Hz to 8 KHz in steps of 50 Hz or 100 Hz. At each frequency the two voltages and phase angle between them were recorded. From these data, experimental pressure ratio was calculated by using Equation (2.32). A digital computer program was designed to calculate theoretical pressure ratio using Equation (2.31). The values of Z_c and τ required for calculation of A_{P1} and B_{P1} are obtained from Equations (2.26) and (2.27). The error in calculations

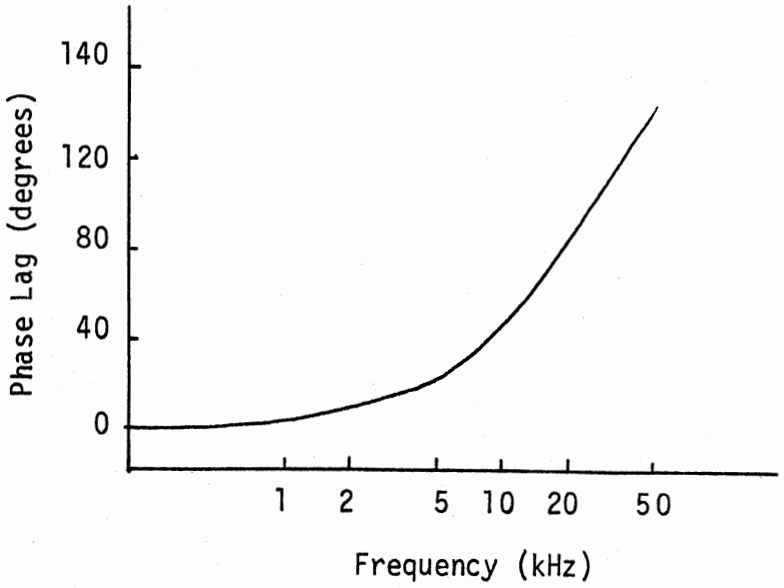

(a) Phase Characteristics of ½-inch Mic.

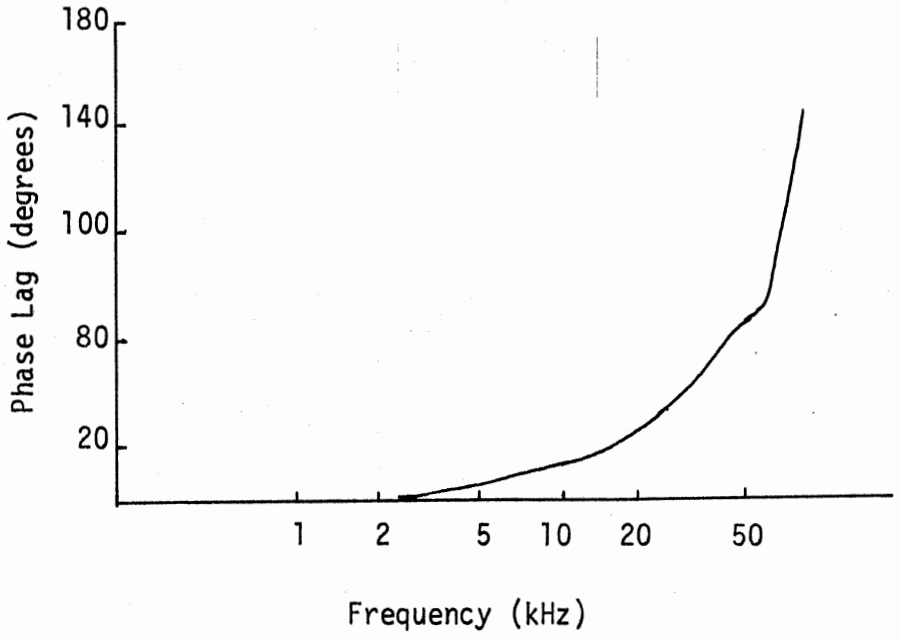

(b) Phase Characteristics of ¼-inch Mic.

Figure 9. Pressure Response and Phase Angle Characteristics of B&K Microphones

of these quantities depends on the errors made in measuring tube dimensions (to which it is most sensitive), and the errors made in measuring air properties such as density, viscocity, temperature, thermal conductivity, etc. A plot of magnitude and phase versus frequency of theoretical and experimental pressure ratio is shown in Figure 10. A close agreement between the two sets of data indicates that the mathematical model of the probe tube is correct. The observed variation can be attributed to various factors such as errors made in measuring tube dimensions, error in microphone impedance and its phase characteristics and inaccuracies in the values of air properties used in calculation of theoretical pressure ratio. However, these errors appear to be small, and the observed variation between theoretical and experimental data is within acceptable limits.

During the course of the experiment, it was observed that for calculation of theoretical pressure ratio, the equivalent length of the tube must be employed. This is expected because the tube under investigation is short and end effects are comparable to its length and hence cannot be neglected. The equivalent length of the tube is obtained by applying end correction to both ends, and is given by (14):

$$L_e = L + 2\,\frac{16R}{3\pi} \tag{2.33}$$

Based on the measurement principle described in this chapter, the instrument to measure the acoustic impedance is designed. The details of the instrument and its experimental evaluation are described in the next chapter.

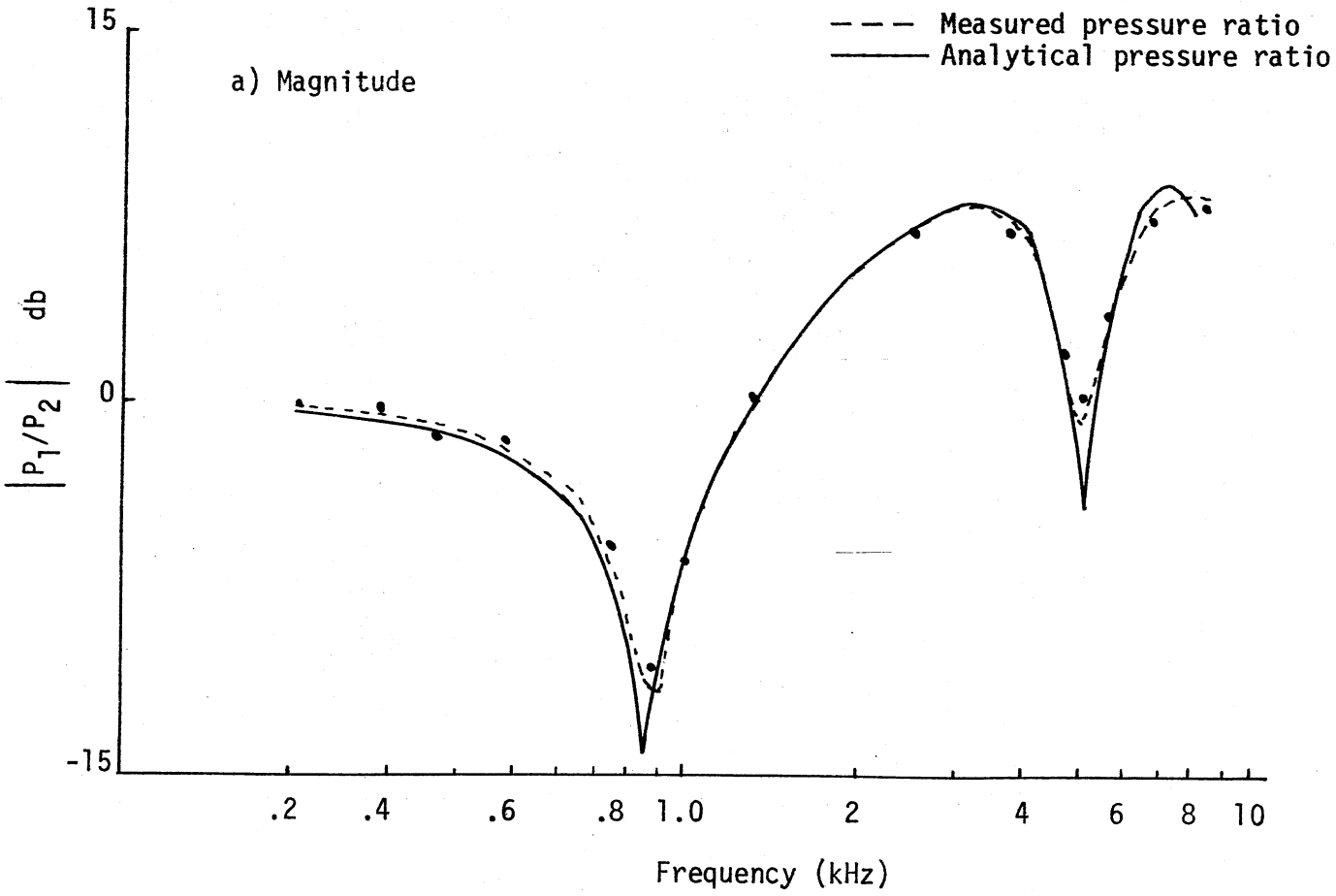

Figure 10. Theoretical and Experimental Pressure Ratio

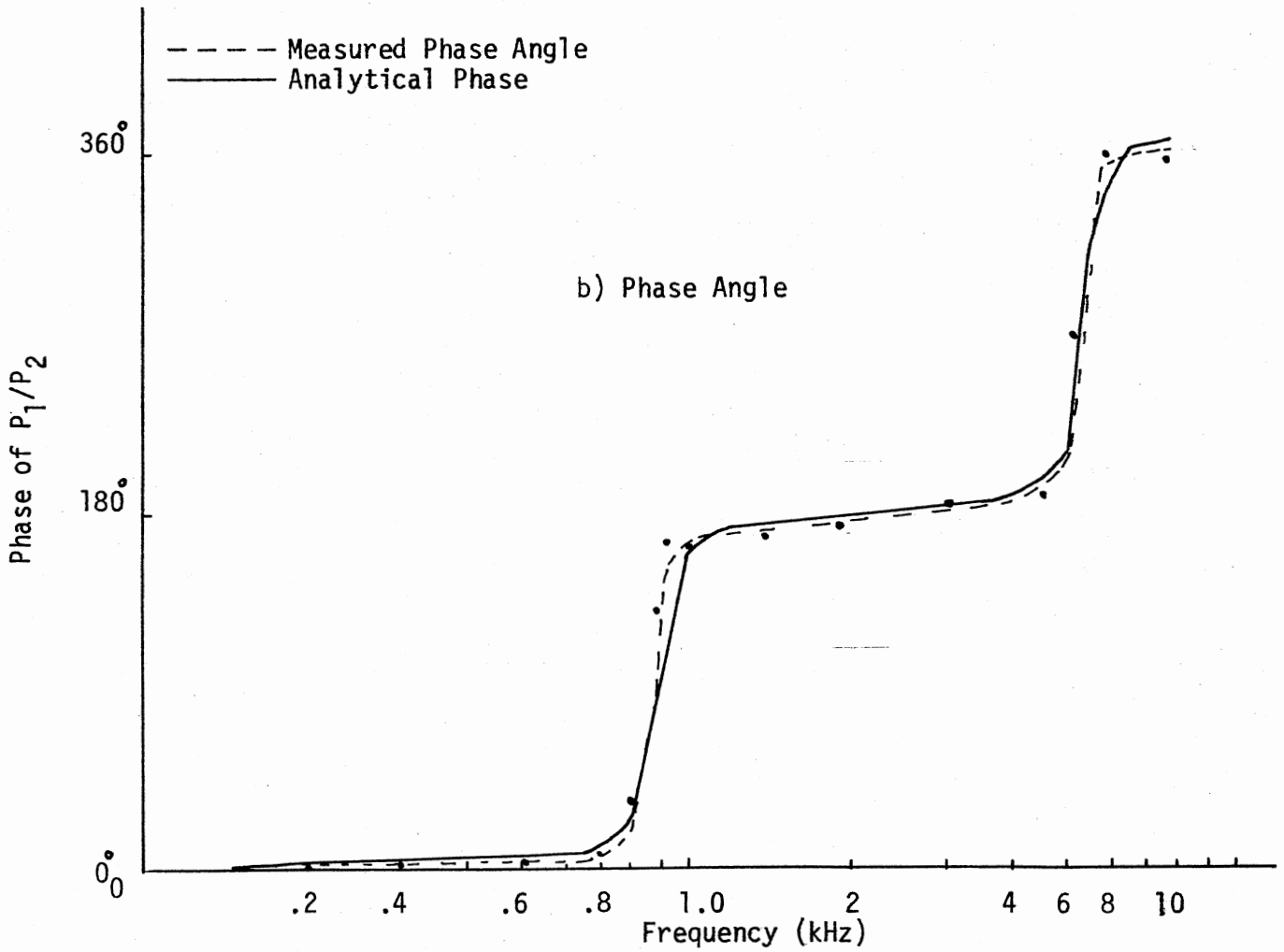

Figure 10 (continued)

CHAPTER III

THE IMPEDANCE-MEASURING INSTRUMENT

3.1 Introduction

It was shown in the last chapter that an acoustic impedance connected to the end of a tube can be found by measuring pressures at two points on the tube and using the sound propagation parameters of the tube. Based on this principle, the impedance-measuring instrument has been designed. The subject of design of the instrument and its experimental validation is discussed in the present chapter.

3.2 Design of the Instrument

The impedance measurement technique described earlier amounts to measuring pressures at two points on a tube connected to an unknown impedance, as shown in Figure 11. The parameters to be selected while designing the instrument are: (a) the distance L_1 between the points P_1 and P_2 where the pressures are measured; (b) distance L_2 between point P_2 and the unknown impedance, and (c) radius of the impedance tube R. If the instrument were to be designed to measure the acoustic impedance of an object, these parameters can be arbitrarily selected, since the measurement principle does not impose any restrictions on their values if the radius of the tube is so selected as not to violate any of the assumptions underlying the distributed parameter model of a tube stated

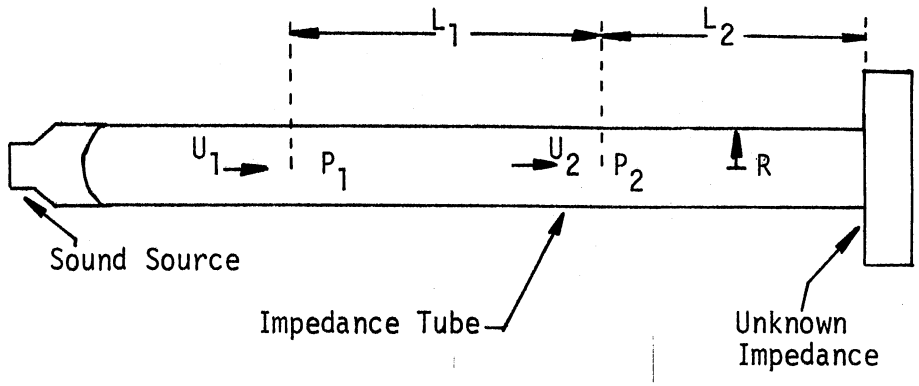

Figure 11. Basic Measurement Scheme and Design Parameters

in Chapter II. The measurement technique would yield accurate results provided the tube dimensions are measured accurately and pressures are measured precisely at two points. But measurement of the acoustic impedance of a human ear presents some unique problems, since the measuring instrument has to satisfy certain constraints. And this requires a systematic procedure to select the design parameters.

Since the static acoustic impedance is the quantity to be measured, the measurements must be carried out in the absence of any middle ear muscle reflexes which are elicited if the sound pressure level in the ear canal exceeds about 80 db. This imposes the first constraint on the instrument which requires the pressure measurement system to be sensitive to pressures below 80 db. Low pressure measurement systems usually have a loading effect that disturbs the sound field inside the impedance tube. This effect can be minimized by carefully choosing the design parameters mentioned above.

The second constraint on the selection of the design parameters is imposed by the requirement for a small instrument. A small instrument that can be fixed on a headset and can be handled easily is desired. Such a mounting arrangement would eliminate any tension that would be caused by mounting the instrument on a fixed rigid frame and requiring the subject to sit in one position until the measurements are complete.

In the following sections, a step-by-step design procedure for the instrument satisfying the above constraints is presented.

3.2.1 Impedance Tube Diameter

In the impedance measurement of a human ear, connecting the measuring instrument to an ear canal poses a difficult problem. For

accurate measurements, it is absolutely necessary to have a good acoustic seal. This is achieved by fixing an appropriately sized ear plug made of soft material on the tip of the impedance tube. This requires that the diameter of the impedance tube and surrounding ear plug be small enough to allow its insertion in the ear canal. Since the average diameter of the ear canal is about 7 mm, a tube of 4 mm outside diameter and 3.2 mm inside diameter is selected to serve as an impedance tube. For this tube, the assumptions underlying the distributed parameter model stated in Chapter II (page 18) are not violated.

3.2.2 Pressure Measurement Scheme

Having selected the diameter of the impedance tube, the next objective is to devise a scheme to measure pressures at any two points on the tube. Factors deciding the distance between these points will be discussed later in the chapter.

The results of the experiment described in the last chapter showed that the mathematical model of the tube was very sensitive to errors in measurement of tube dimensions. It is therefore necessary to measure pressures precisely at two points on the tube for accurate measurement of impedance. This is achieved by the pressure measurement scheme shown in Figure 12.

Two probe tubes are inserted in the small cavities created at the points on the tube where the pressures are to be measured. The probes are so mounted that their ends are in flush with the walls of the cavity, ensuring that the pressures are measured exactly at two points separated by distance L_1. The probe tubes are connected to 1/2 in B&K microphones. A spacer is provided between the probe tube and the

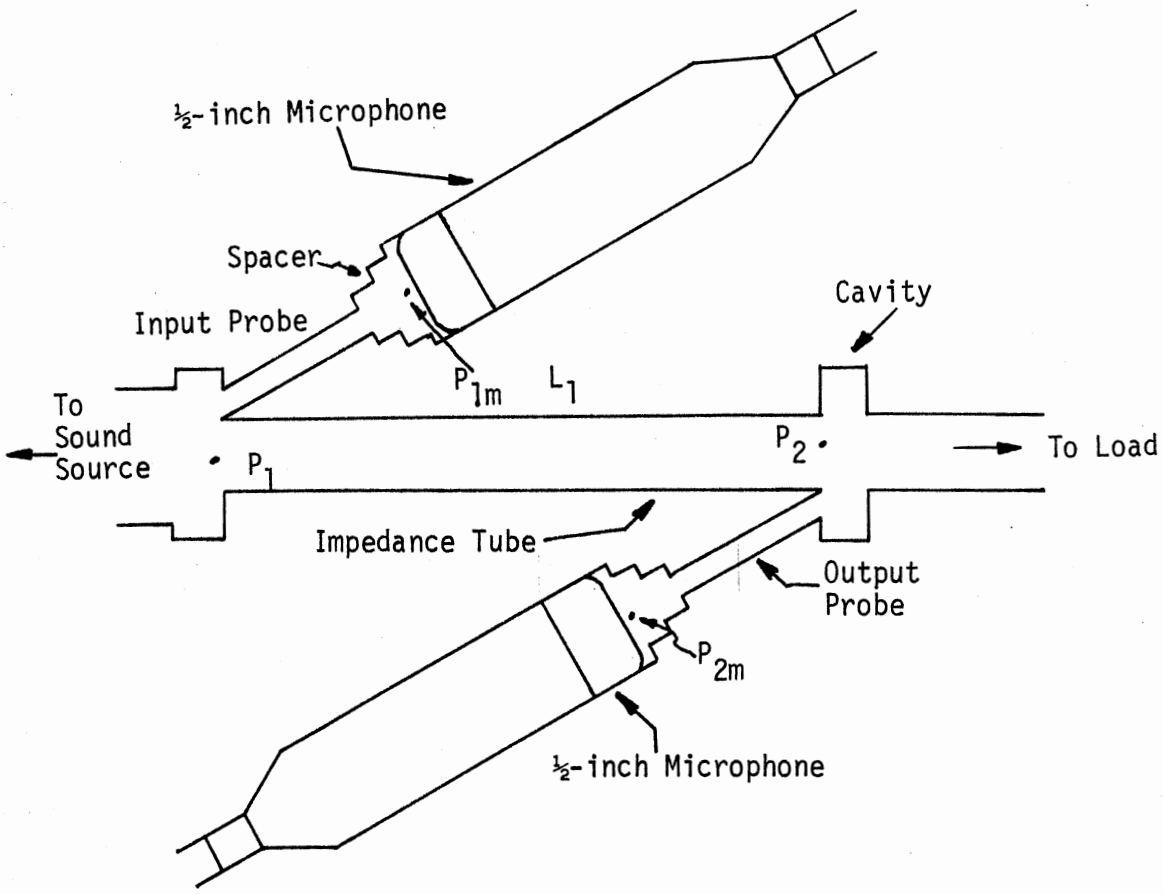

Figure 12. The Pressure Measurement Scheme

microphone diaphragm for the reasons mentioned in Chapter II. The pressure measurement scheme described here, however, requires modeling of the probe tubes in order to relate the pressures measured by the microphones to the actual pressures existing at the entrance to the probe tubes.

The task of modeling the probe tubes could be avoided if small microphones were inserted directly into the cavities instead of the probes. This was not done here for two reasons. First, the sensitivity of a small microphone is low and small changes in pressure may remain undetected. Second, the dynamic range of the small microphones which are currently available (B&K 1/8-inch microphone) is 70 db to 180 db. As mentioned earlier, during the impedance measurement process, the sound pressure level in the ear canal should be kept below 80 db to prevent reflexive contractions of the middle ear muscles. So small microphones would be operating at its lowest level of dynamic range and the signal to noise ratio would be small. The ½-inch microphones connected to the probes have much wider dynamic range and better sensitivity.

3.2.3 Effect of Probe Tube

In the last chapter, the relationship between two pressures at sections 1 and 2 on the impedance tube and the impedance at section 2 were derived. Recalling this equation,

$$Z_2 = B_1/(R'-A_1) \tag{2.20}$$

In deriving this equation, it was assumed that pressures are measured by some device, and no consideration was given to the effect of the presence of pressure measuring device on the sound field in the

tube. In the present investigation, since the probe tubes are used to measure pressures, there are two problems that deserve consideration.

First, since the microphone measures pressure at the exit end of the probe tube, the equation must be obtained to relate this measured pressure to the pressure existing at the entrance to the probe tube. This relationship was derived in Chapter II in connection with the probe tube experiment. It was shown that if P_1 and P_{1m} are the pressures at the entrance to the probe tube and the pressure measured by the microphone at the exit end of the tube, they are related by

$$P_1 = (A_{P1} + B_{P1}/Z_{mic}) * P_{1m} \tag{2.31}$$

where A_{P1} and B_{P1} are the equivalent four-pole parameters of the probe tube and Z_{mic} is the acoustic impedance of the microphone. The probe tube used in that experiment is employed to measure pressure P_1 on the impedance tube of the instrument. In the following discussion, this probe tube is referred to as the input probe tube. Similarly, the probe that measures pressure P_2 on the impedance tube is referred to as the output probe tube.

From the experimental results shown in Figure 10, it is observed that a large discrepancy appears between the theoretical and experimental values of the pressure ratio in the frequency band of 700 Hz to 1100 Hz, and the maximum error occurs at 900 Hz, which is the first resonant frequency of the probe tube. Hence, this probe cannot be used in this frequency band and a probe of different length must be employed. In the present investigation, a probe six centimeters long is employed because the resonant frequency of this probe is much lower than that of the previous probe. The experiment similar to one described in Chaper

II was conducted on this probe. The theoretical and experimental pressure ratio for this probe as a function of frequency is shown in Figure 13. It is observed that in the frequency range of 700 Hz to 1100 Hz where the first probe cannot be used, the experimental and theoretical data are in good agreement for the six centimeter long probe.

The equation similar to Equation (2.31) can be written for the output probe tube as follows:

$$P_2 = (A_{P2} + B_{P2})Z_{mic} * P_{2m} \tag{3.1}$$

where A_{P2} and B_{P2} are the equivalent four-pole parameters of the output probe tube. The discussion on the selection of the output probe tube is presented later in this chapter.

The pressure ratio R' that appears in Equation (2.20) can now be written as

$$R' = \frac{P_1}{P_2} = \frac{A_{P1} + B_{P1}/Z_{mic}}{A_{P2} + B_{P2}/Z_{mic}} \cdot \frac{P_{1m}}{P_{2m}} \tag{3.2}$$

The second problem caused by the probe tubes used for pressure measurement is concerned with their effect on the sound field in the impedance tube. The probe tube has a finite input impedance which causes loss of volume velocity at the section where it is introduced to measure pressure. In order to analyze this effect, the measuring instrument is divided into two segments, as shown in Figure 14a. The portion of the instrument between sections 1 and 2 constitutes the first segment. The second segment consists of a cavity to the right of section 2 with the part of the impedance tube that leads to the unknown impedance.

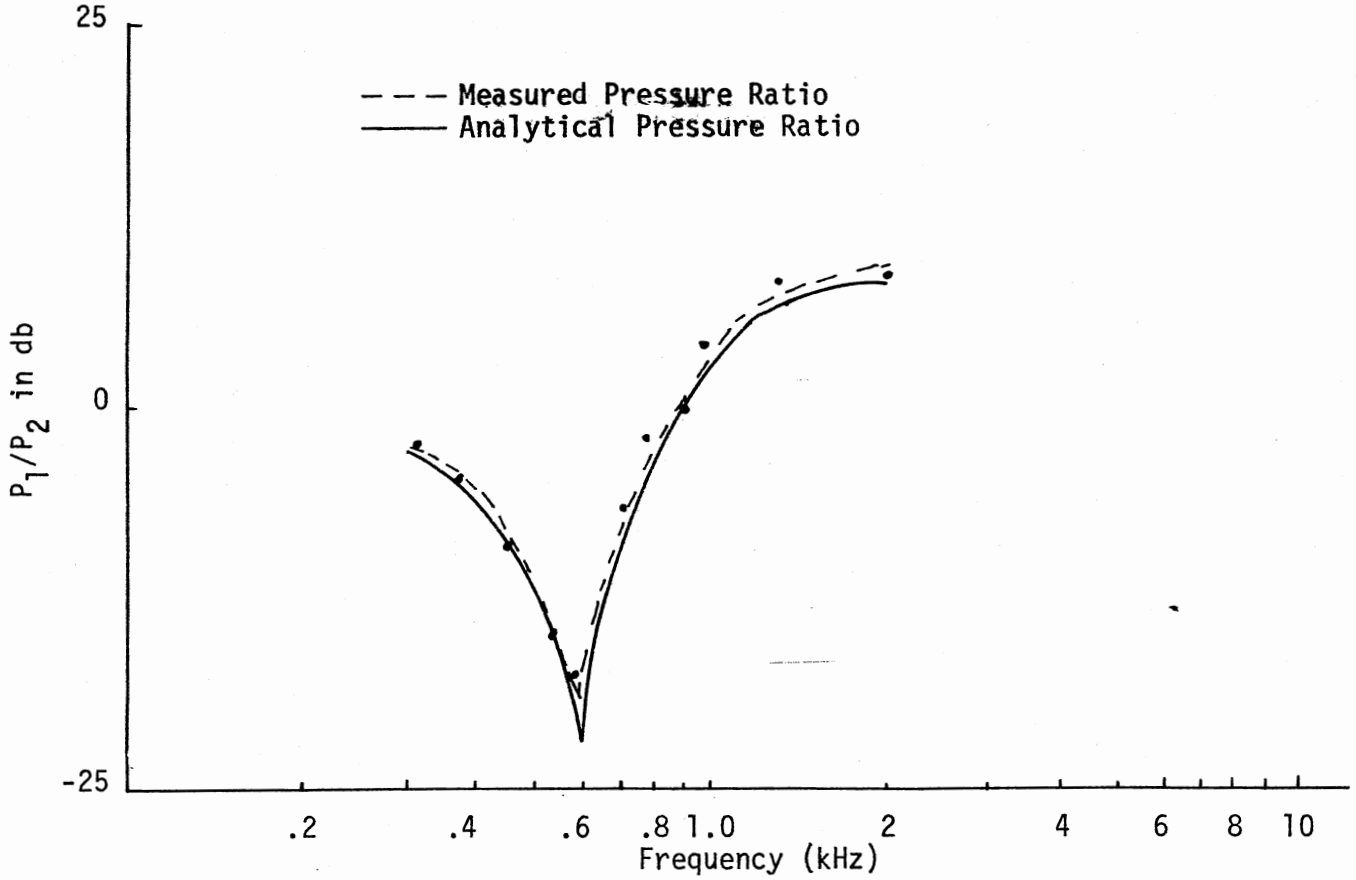

Figure 13. Theoretical and Experimental Pressure Ratio for Six Centimeters Long Probe Tube

With reference to Figure 14(a), the total volume velocity at section 2 can be written as

$$U_2 = U_P + U_{in} \tag{3.3}$$

where U_P and U_{in} are volume velocities input to probe tube and segment 2, respectively. In terms of impedances, equation (3.3) can be written as

$$P_2/Z_2 = P_2/Z_P + P_2/Z_{in} \tag{3.4}$$

where Z_P and Z_{in} are the input impedances of probe tube and segment 2, respectively. Equation (3.4) can be solved for Z_{in}, and the result is

$$Z_{in} = Z_P * Z_2/(Z_P - Z_2) \tag{3.5}$$

Once Z_{in} is obtained, the unknown impedance can be calculated by using the four-pole model of segment 2 and Equation (2.25).

From the above development, it can be seen that the input impedance of the probe tube measuring pressure P_1 has no effect on the measurement.

Although the effect of loading due to the finite input impedance of the probe tube is taken into account in determining the unknown impedance, in actual measurement large errors can be expected in situations where the probe impedance is much smaller than Z_{in}, the input impedance of segment 2. This situation is shown in Figure 14(b).

For $Z_P << Z_{in}$, calculated impedance Z_2 is almost equal to Z_P. This causes the quantity $(Z_P - Z_2)$ to approach zero. Thus, any errors made in calculating Z_P and Z_2 appear magnified in the unknown impedance

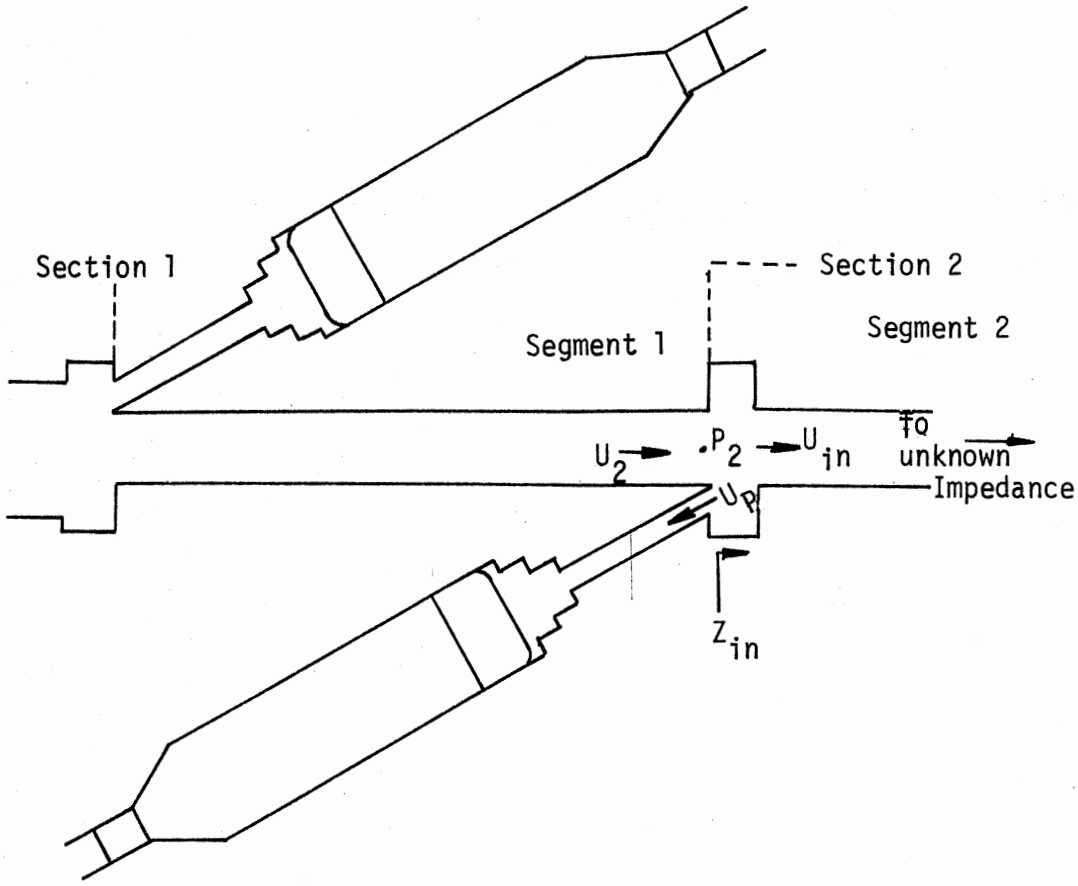

(a) Loading due to Probe Tube

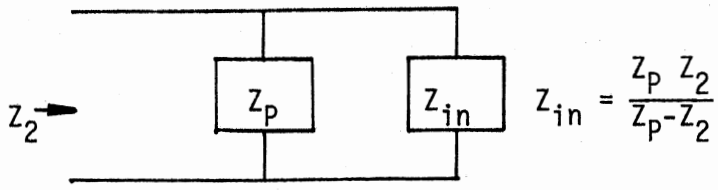

(b) Impedance Seen at Section 2

Figure 14. Effect of Finite Input Impedance of Probe Tube

calculations. This problem demands a closer look at the impedance profile of the output probe tube.

A schematic diagram of the output probe tube with a spacer and its equivalent four-pole network was shown in Figure 6. The input impedance of the probe is calculated using the following equation:

$$Z_P = (A_{P2} * Z_{mic} + B_{P2})/(C_{P2} * Z_{mic} + D_{P2}) \qquad (3.6)$$

A plot of absolute value of Z_P versus frequency is shown in Figure 15. At the reasonant frequencies of 980 Hz and 5800 Hz, the input impedance is very low.

Now consider, for example, a situation where this probe is employed to measure pressure P_2, and the input impedance of segment 2, Z_{in}, is 300 egs units. Then from Figure 15 it can be seen that in the frequency rangesof 490 Hz to 1600 Hz and 500 Hz to 6500 Hz, Z_P is smaller than Z_{in}, and therefore large errors in impedance measurement may be expected. In other words, this probe can be used only in the frequency range excluding the above bands.

The above discussion leads to the conclusion that a single probe cannot be used over the entire frequency range of interest. Moreover, the usable frequency range for a particular probe depends on the input impedance of segment 2 (Z_{in}) which, in turn, depends on the unknown impedance to be measured.

In the present investigation, four different probes are used to cover the frequency range up to 8 kHz. The lengths of the probes are selected in such way that their resonant frequencies are evenly spaced over the frequency range of interest. The input impedance of each probe is calculated by using Equation (5.6). Its absolute value is

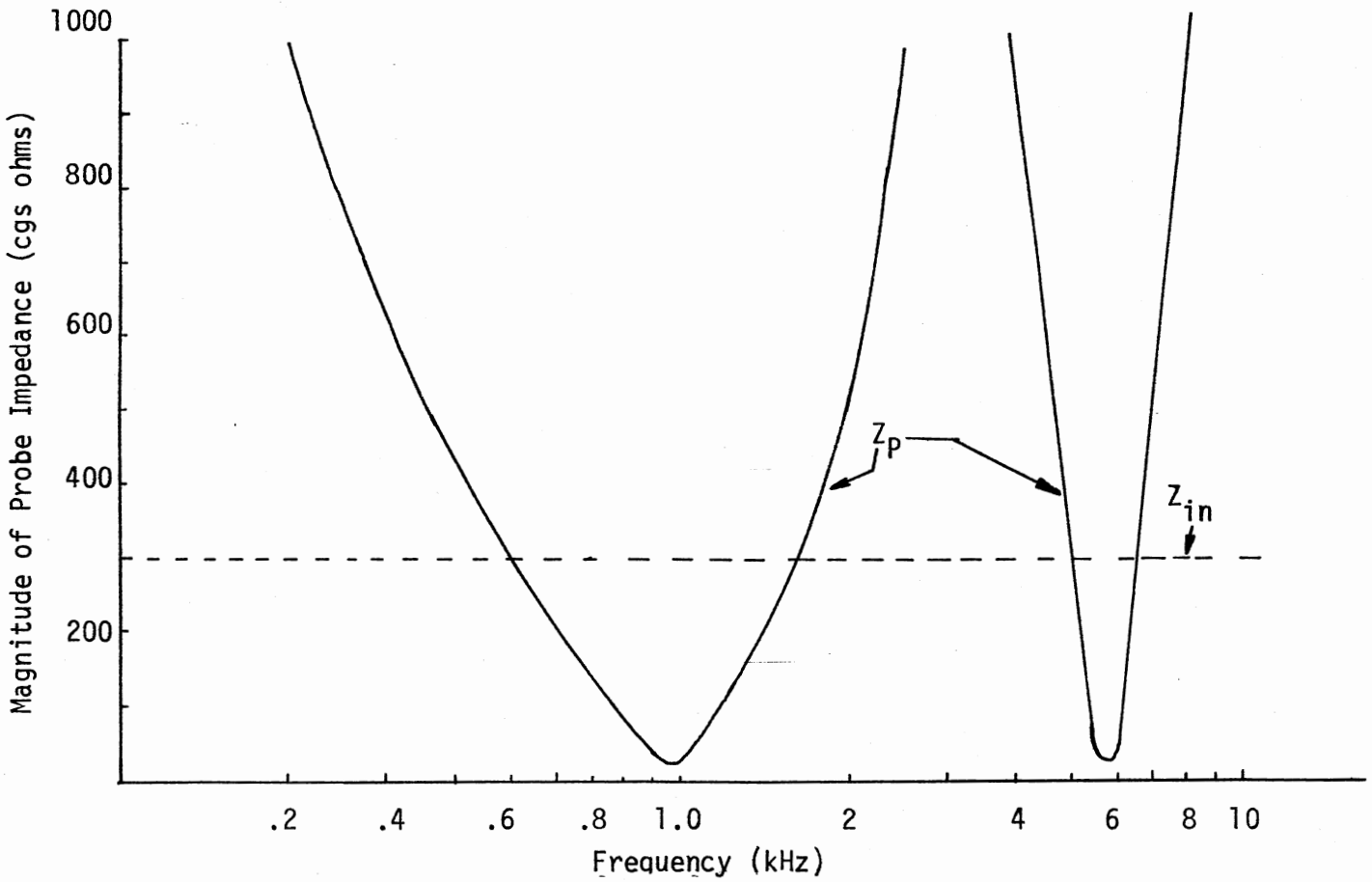

Figure 15. Input Impedance Profile of the Probe Tube

plotted as a function of frequency as shown in Figure 16. From this figure, the probe tube with the highest input impedance and the frequency range over which it can be used is decided. The results are presented in the following table.

TABLE I

LENGTHS AND OPERATING FREQUENCY RANGES OF THE PROBE TUBES

Probe Length (cm)	Frequency (Hz)
2.62	100 - 500 2200 - 3800
4	5200 - 7000
6	1100 - 2100 3900 - 4800
14	500 - 1000

These results are also shown in Figure 17, where input impedance of the probe and its usable frequency range is indicated. As long as the input impedance of segment 2 falls below the curve shown in Figure 17, accurate impedance measurement can be expected.

For each of the four probes, the experiment described in Chapter II is performed, and theoretical and experimental pressure ratios are calculated over the usable frequency of the corresponding probe. The results are shown in Figure 18. It can be seen that the two sets of

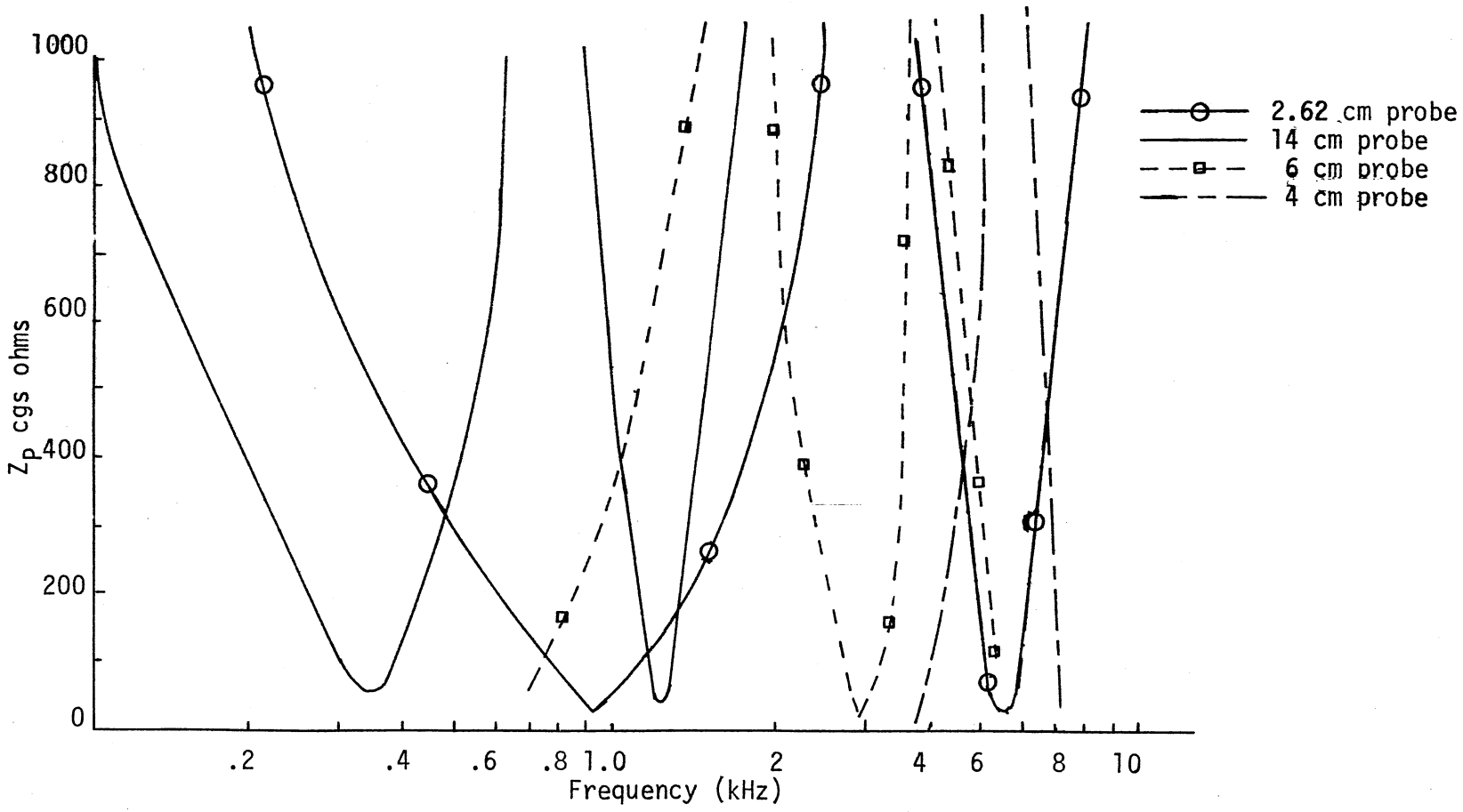

Figure 16. Input Impedance of Different Probe Tubes

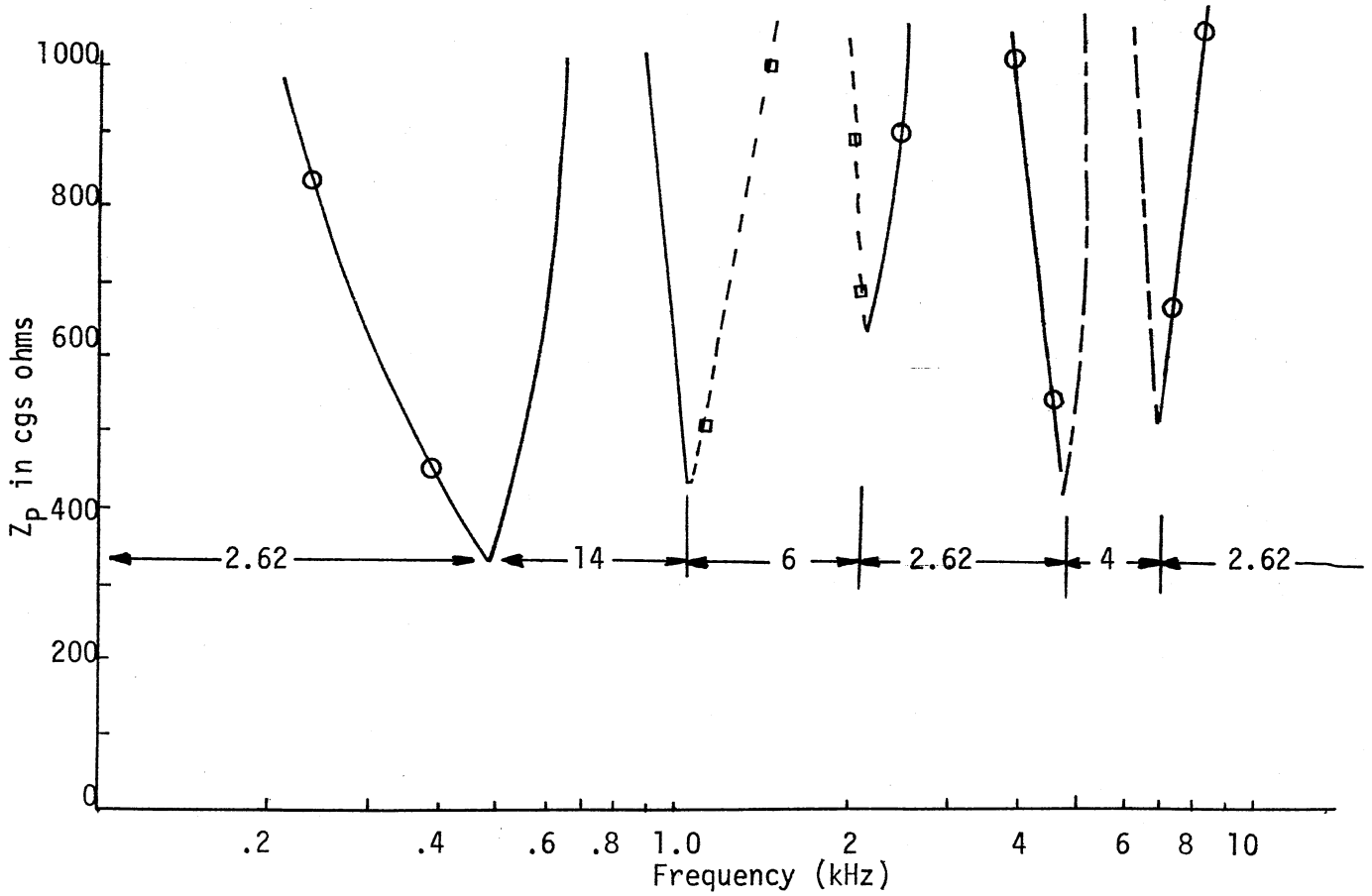

Figure 17. Input Impedance of Selected Probe Tubes and Their Usable Frequency Range

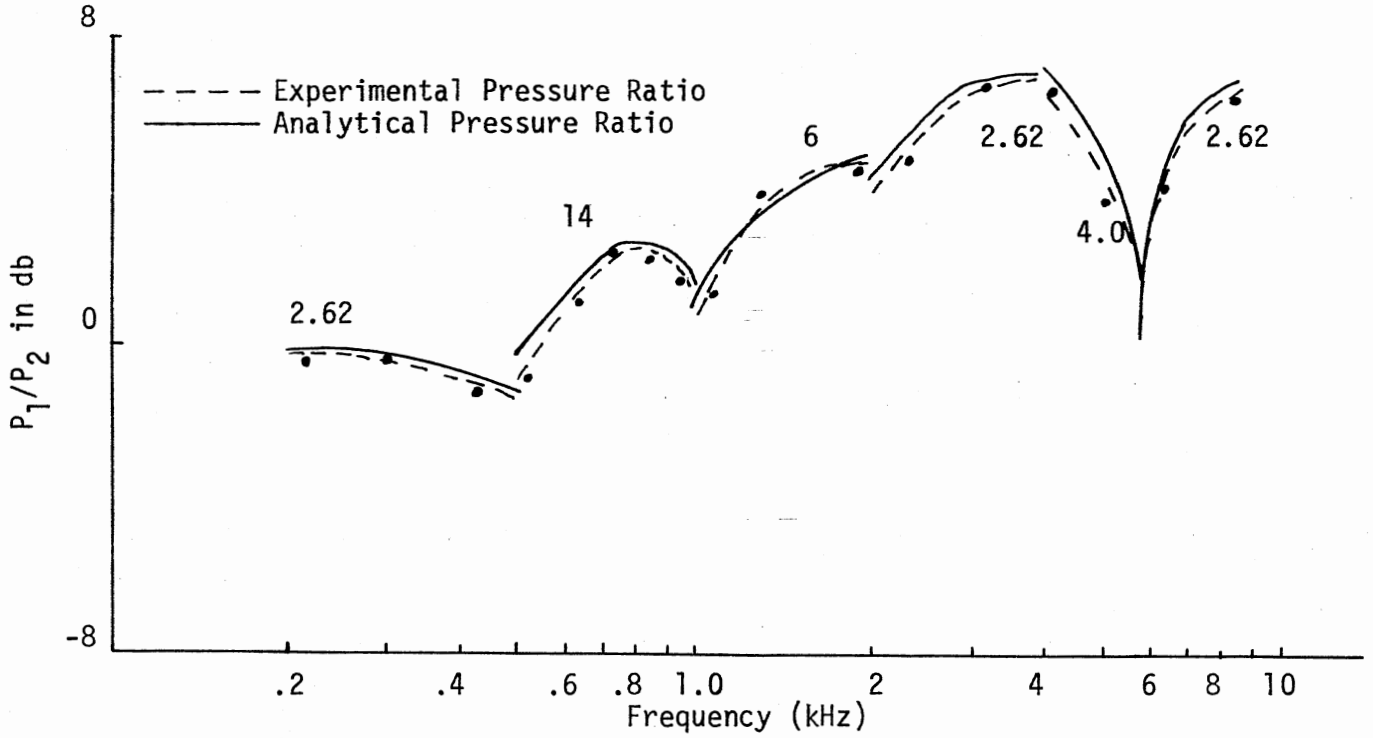

Figure 18. Theoretical and Experimental Pressure Ratios for Selected Probe Tubes

data are in good agreement. The observed variation can be attributed to errors made in measuring tube dimensions, air properties, microphone impedance, etc.

3.2.4 The Complete Instrument

A schematic diagram of the parts of the instrument is shown in Figure 19. Segment 1 of the instrument has three parts--a middle cylinder with two end connectors that can be screwed on either end. A 3.2 mm-diameter hole is drilled through the longitudinal axis of all three pieces. With this arrangement, length L_1 of a segment 1 can be changed if desired by inserting the middle cylinder of a different length. The end connectors support the probe tubes. Holes are drilled in both the end connectors at an angle so that a probe tube with a spacer and ½-inch B&K microphone can be properly positioned.

Segment 2 of the instrument consists of a cylindrical piece that forms the cavity at section 2 and the part of the impedance tube of length L_2 that leads to the unknown impedance. The diameter of the cavity is so selected that its inside surface is tangent to the probe tube opening in the end connector, as shown in Figure 19.

A complete sketch of the instrument with the two segments connected and with the microphones connected to the probe tubes is shown in Figure 20.

For proper connection of the instrument to an ear canal, the impedance tube of segment 2 (of length L_2) should be longer than 7 cm. This would provide sufficient room between the input probe microphone and the subject's head. Having selected L_2, the only dimensions to be chosen are the length of the cavity and the length of segment 1.

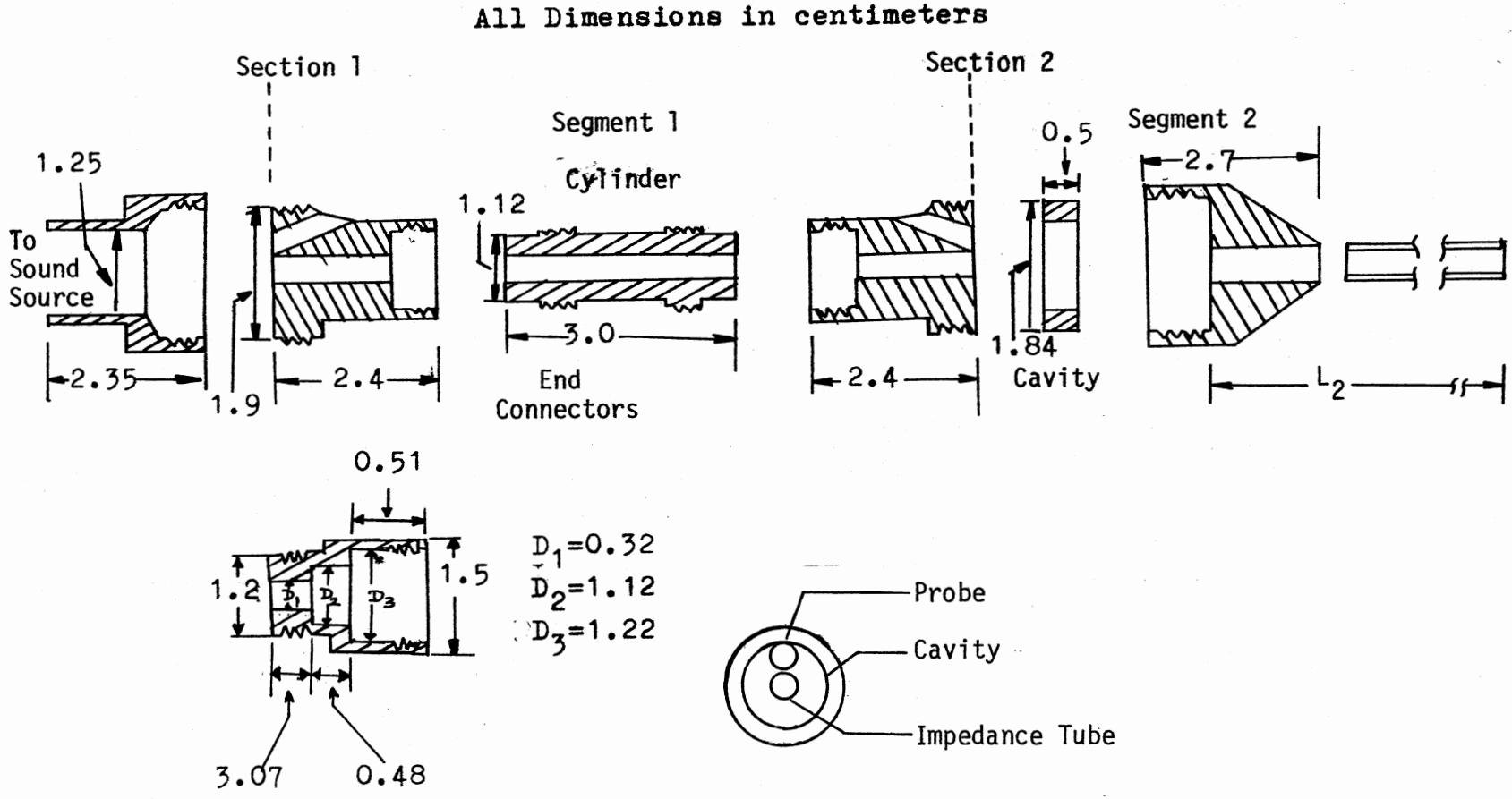

Figure 19. Components of the Measuring Instrument

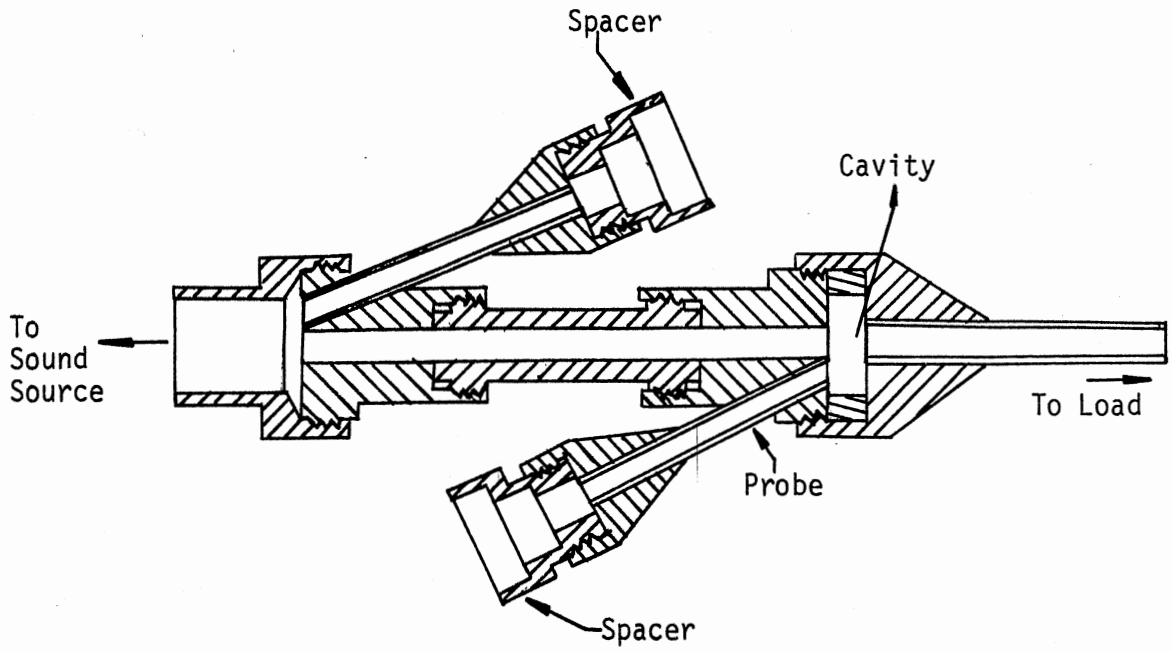

Figure 20. The Complete Instrument

Factors affecting selection of these parameters are discussed in the following sections.

3.2.5 Length of the Cavity

A schematic diagram of segment 2 is shown in Figure 21(a). For the purpose of discussion, the segment is represented by a parallel combination of Z_{CV} and Z_3, representing the impedance of the cavity and impedance of section 3, respectively, in Figure 21(b). The input impedance of the segment can then be written as

$$Z_{in} = Z_{CV} * Z_3 / (Z_{CV} + Z_3) \tag{3.7}$$

It was shown in section 3.2.3. that for accurate measurements, the input impedance of segment 2 and that of the probe tube must satisfy the folowing constraint

$$Z_{in} < Z_P \tag{3.8}$$

From Equation (3.7) it can be seen that Z_{in} is always smaller than Z_{CV}. Therefore, if Z_{CV} is selected so that it falls below the impedance profile of the probe tube shown in Figure 18, the above constraint is always satisfied.

In Figure 22 is shown the impedance profile of the probe tube and that of the cavity of length 0.5 cm. It can be seen that at high frequency, the impedance of the cavity is very low and it has the effect of short-circuiting the load impedance. This requires a smaller cavity for high frequencies. The impedance profile for a small cavity of length 0.3 cm is also shown in the figure. This impedance profile

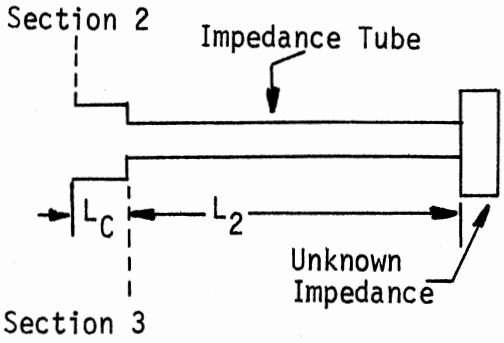

(a) Schematic of Segment 2

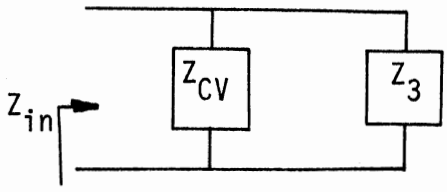

(b) Equivalent Impedance Diagram

Figure 21. Segment 2 and Its Representation by Lumped Impedances

intersects the profile of Z_p at 1200 Hz. Hence, for frequencies above 1200 Hz, the smaller cavity is employed.

3.2.6 Length of Segment 1

As discussed previously, segment 1 consists of two end connectors and a middle cylinder. Since the lengths of the end connectors are fixed, the length of segment 1 can be changed by choosing a middle cylinder of proper length.

The factors considered in selecting the length of segment 1 are: (1) to keep the overall length of the instrument as small as possible; (2) to allow sufficient room between the input probe microphone and the subject's head when the instrument is fixed on the headset, and (3) frequency considerations discussed above.

The general guidelines for its selection can be drawn by studying Equation (2.20) derived in Chapter II relating the two pressure measurements to the impedance at section 2 of the instrument. Recalling this equation,

$$Z_2 = B_1/(R' - A_1) \tag{2.20}$$

where A_1 and B_1 are the four-pole parameters of segment 1 and R' is the pressure ratio.

This equation suggests that B_1 should be of the same order of magnitude or greater than Z_2, for if $B_1 < Z_2$, then $(R - A_1) < 1$ and dividing by a quantity smaller than one would magnify the errors made in measurement.

In the present case, Z_2 is approximately equal to Z_{CV}, the impedance of the cavity. Therefore B_1 should be greater than Z_{CV}.

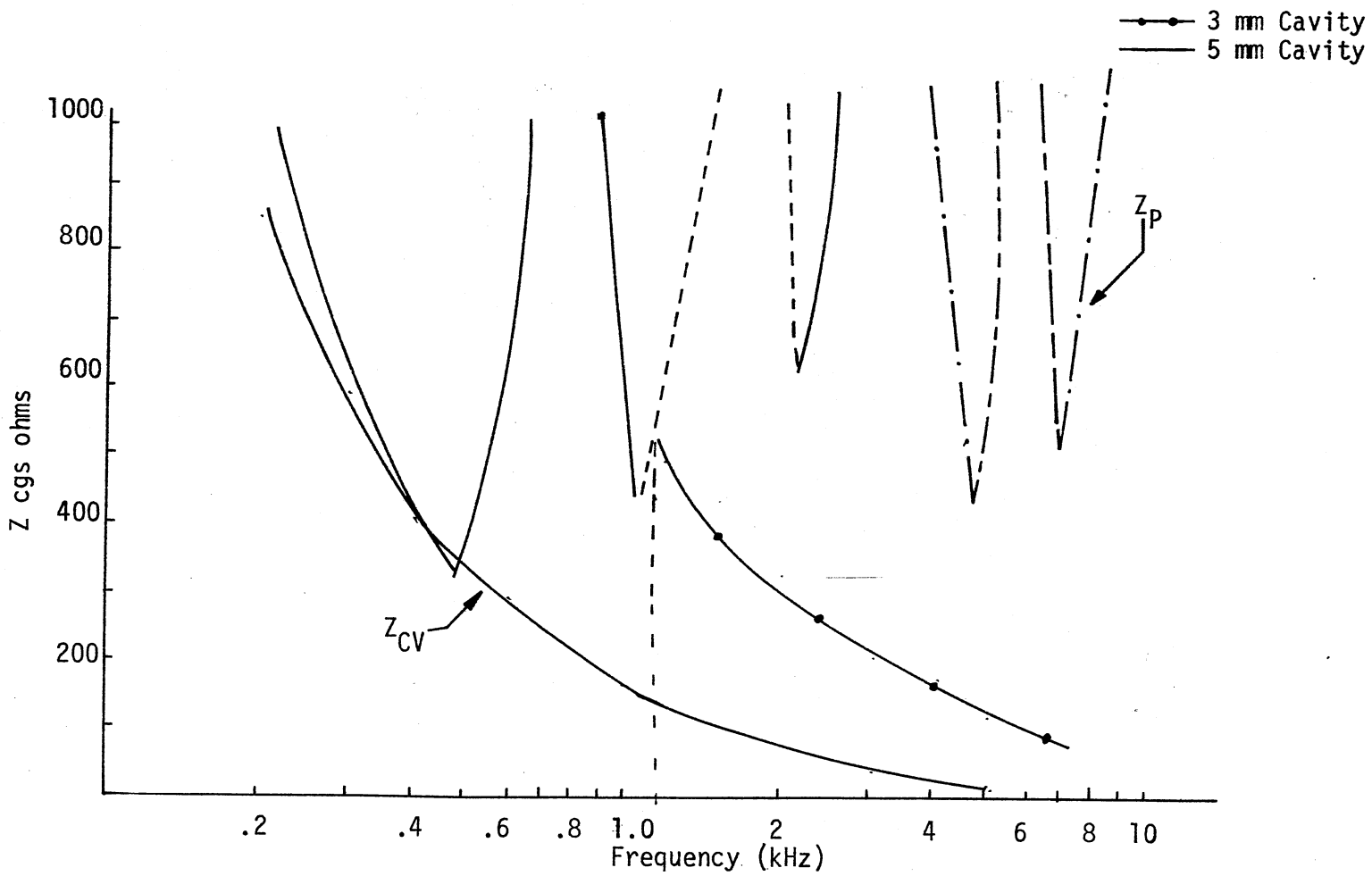

Figure 22. Impedance Profile of Probe Tube and Cavity

In order to satisfy the condition $B_1 > Z_{CV}$, the length of the segment is selected to be 6 cm. This requires the middle cylinder to be 3 cm long. A graph of the magnitude of B_1 versus frequency is also shown in Figure 23. It can be seen that $B_1 > Z_{CV}$ over the frequency range of interest.

3.3 Experimental Validation

Having completed the design and development of the instrument, its performance is checked by taking measurements of standard impedances. The acoustic elements shown in Figure 24 are used for this purpose. The input impedance of these elements is obtained by representing them by a four-pole network model as shown in the figure, and using the equation

$$Z_S = P_{in}/U_{in} = \frac{AP_o + BU_o}{CP_o + DU_o} \tag{3.9}$$

Since the output ends of the elements are blocked,

$$U_o = 0 \tag{3.10}$$

hence

$$Z_S = A/C \tag{3.11}$$

Before Equation (3.11) is used to compute the standard impedance against which the measured impedance will be compared, consideration must be given to the accuracy of the mathematical model of the standard impedance.

The impedance calculated by Equation (3.11) depends on the properties of air such as density, thermal conductivity, viscosity, specific

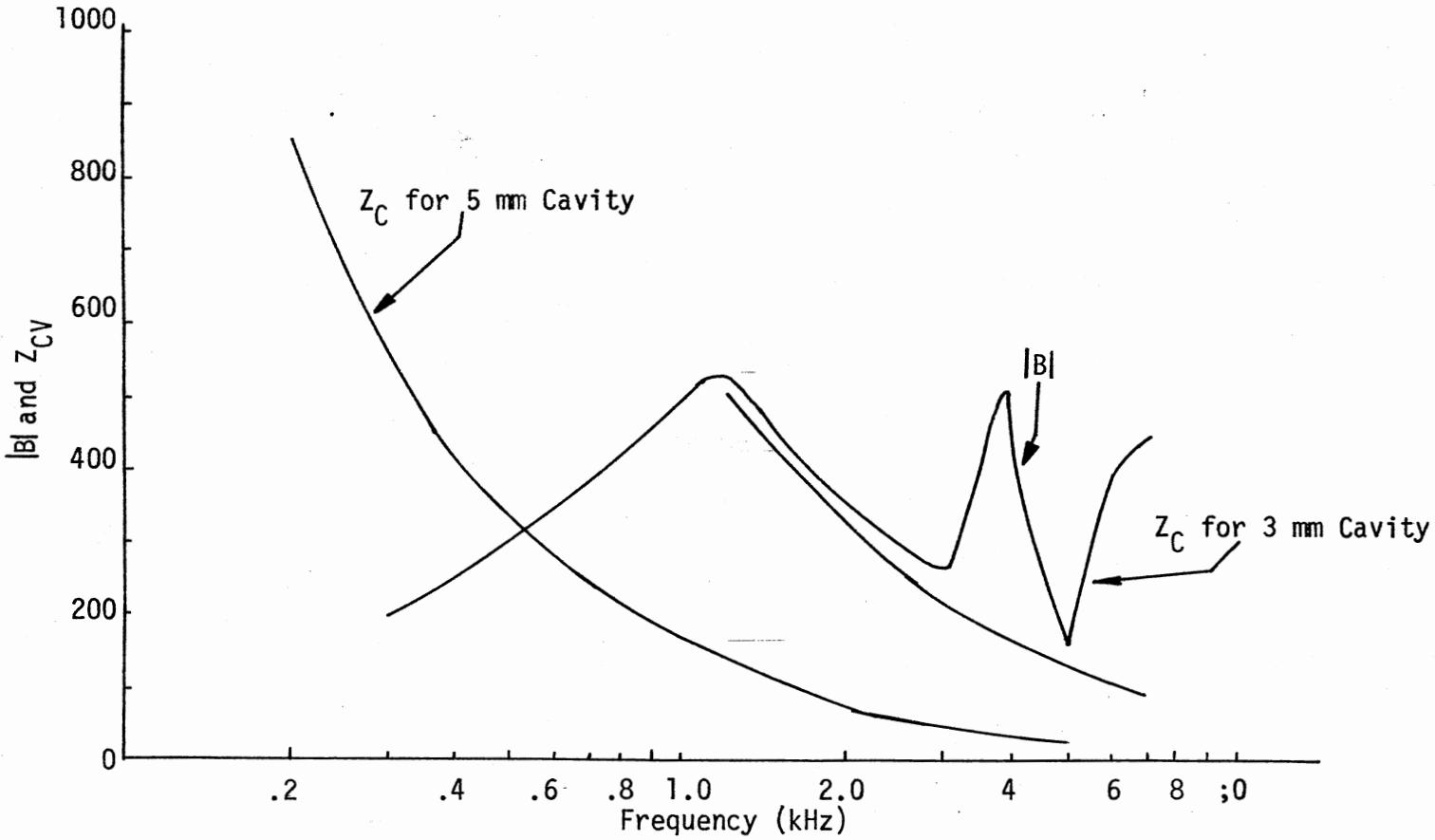

Figure 23. Plot of |B| versus Frequency for Segment 1

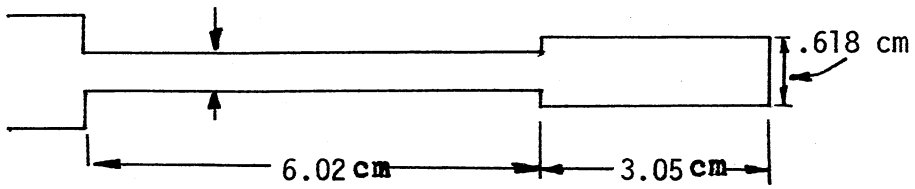

(a) Standard Acoustic Impedance #1

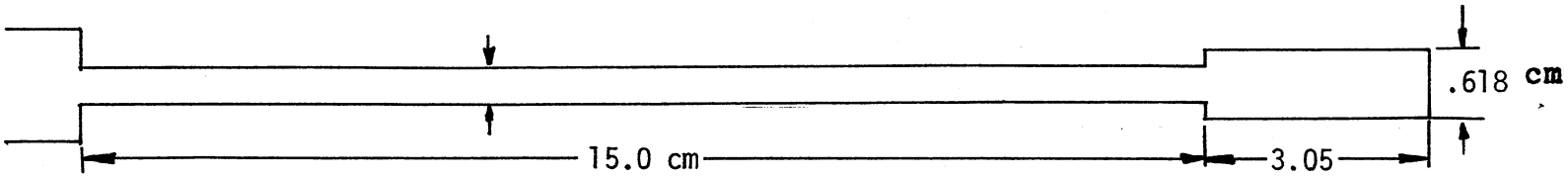

(b) Standard Acoustic Impedance #2

Figure 24. Acoustic Elements Used as Standard Impedances

heats and the dimensions of the acoustic element. In the present study, air properties are obtained from reference 15 and are considered to be accurate. This leaves the effect of errors made in measurement of dimensions to be considered.

For the acoustic elements shown in Figure 24, the dimensions were measured within 0.04 mm. A vernier calliper having a least count of 0.04 mm was employed. In order to obtain the error in standard impedance caused by errors made in measuring tube dimensions, impedance is calculated using Equation (3.11) for the element shown in Figure 24(a), first using the dimensions shown in the figure and then with the dimensions increased by 0.04 mm. A plot of these two impedances versus frequency is shown in Figure 25. From the two values of impedances, maximum error in standard impedance is found to be less than two percent in magnitude and one percent in phase. Similar calculations for other acoustic elements showed the same results. These impedances are then used to check the accuracy of the measured impedance.

The experimental setup used for measurement is shown in Figure 26. Measurements were taken from 100 Hz to 7 kHz in steps of 50 Hz or 100 Hz. At each frequency, microphone voltages and phase angle between them were recorded. From these data, the load impedance was calculated using the equations developed in section 2.2. Plots of measured values of magnitude and phase of the impedances along with their analytical values as obtained from Equation (3.11) versus frequency are shown in Figure 27. It is observed that the maximum error in the impedance measurement lies within twelve percent in magnitude and phase above 1000 Hz and lies within eight percent below 1000 Hz. The major source of error is the inaccuracy in measurement of dimensions of the acoustic

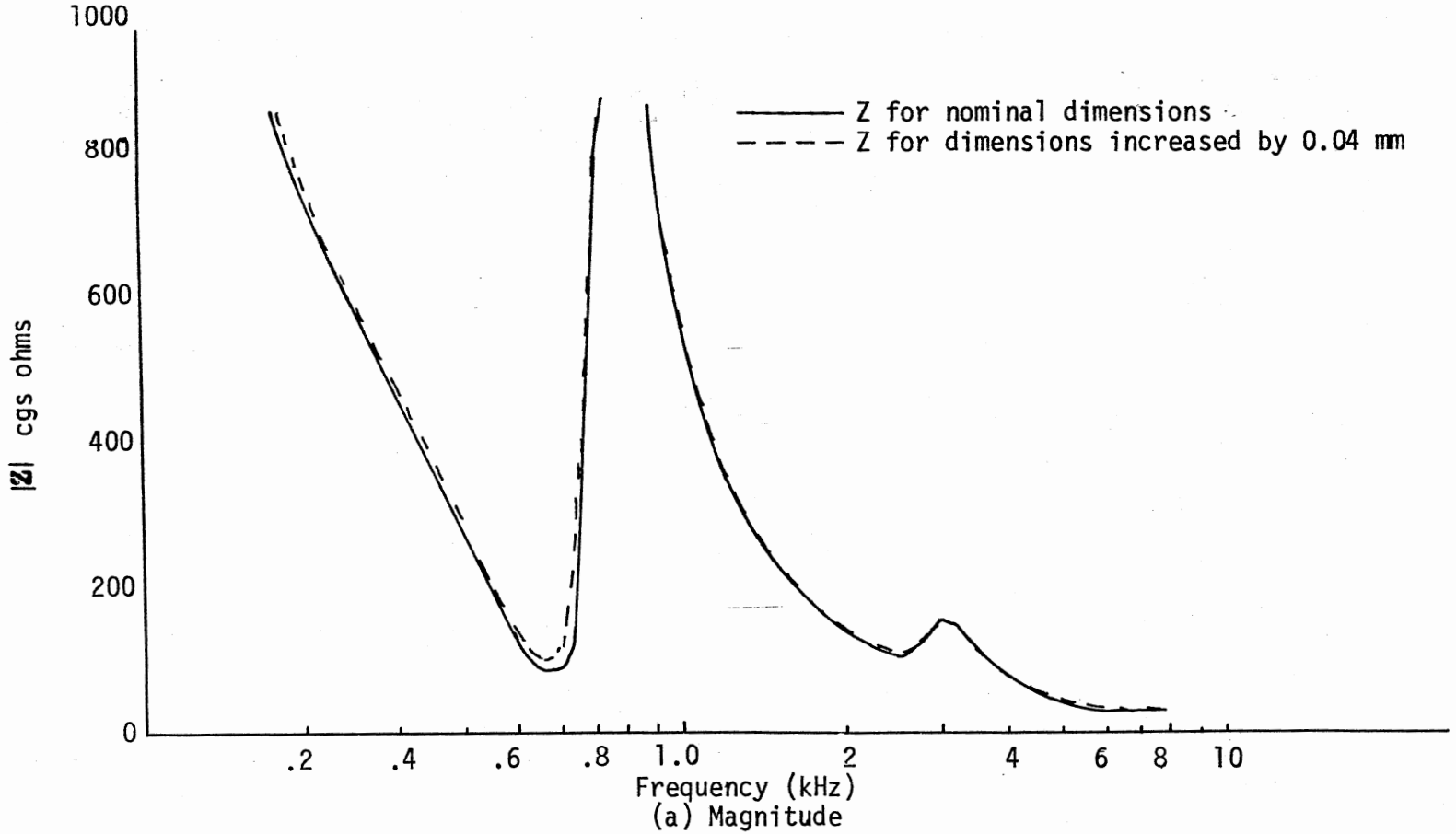

Figure 25. Effect of Change in Dimensions on the Standard Impedance

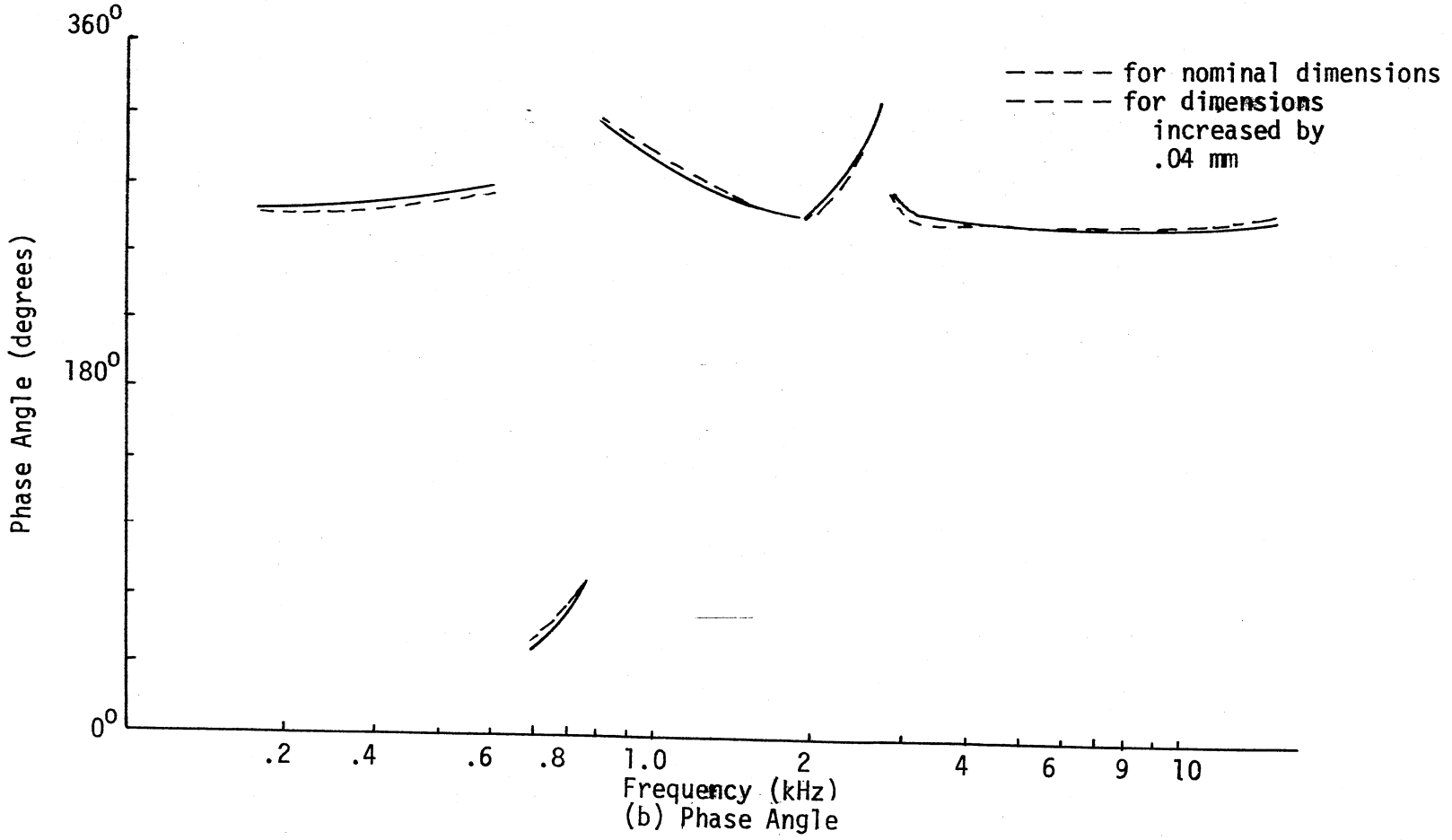

(b) Phase Angle

Figure 25 (continued)

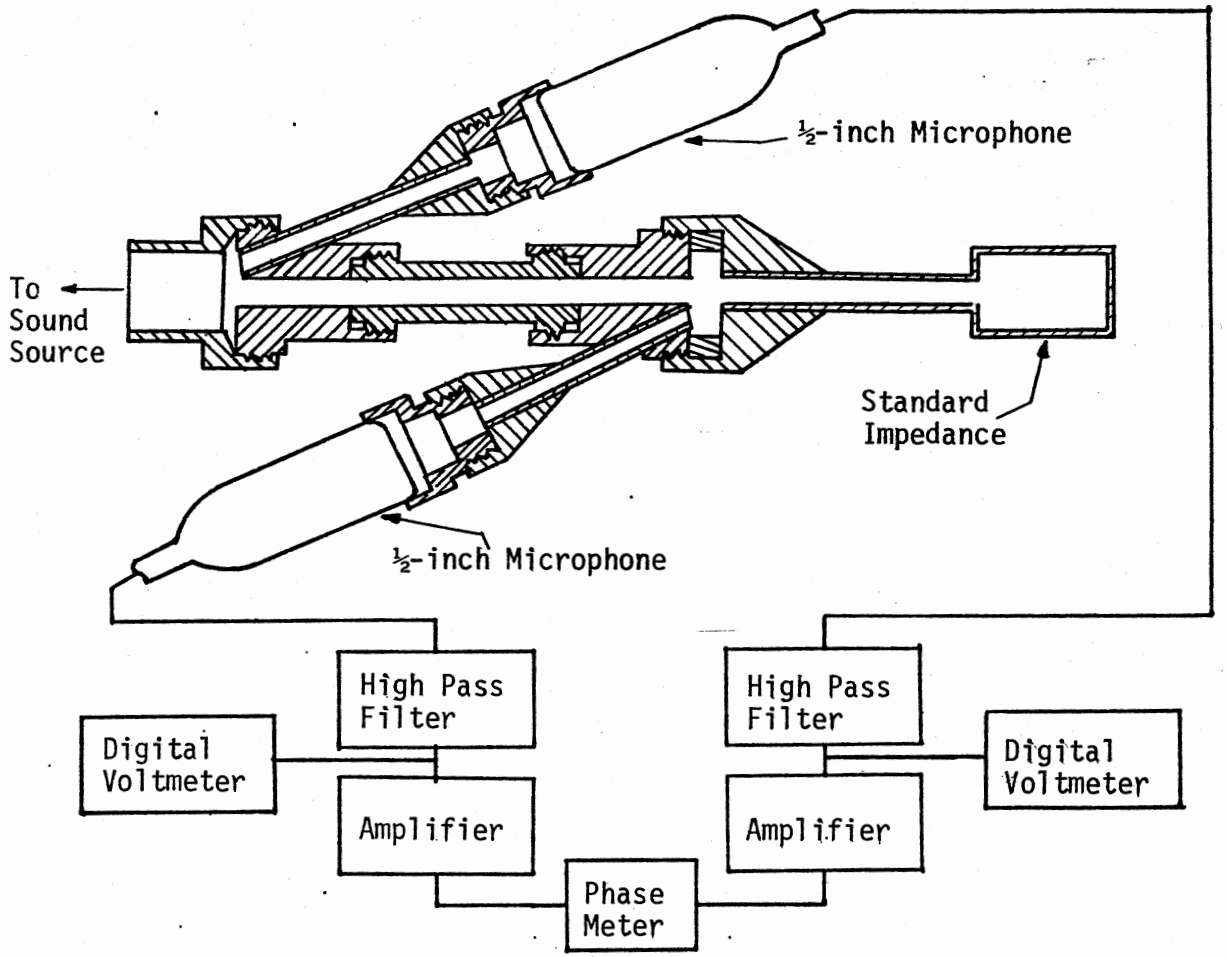

Figure 26. Experimental Setup to Measure Standard Impedances

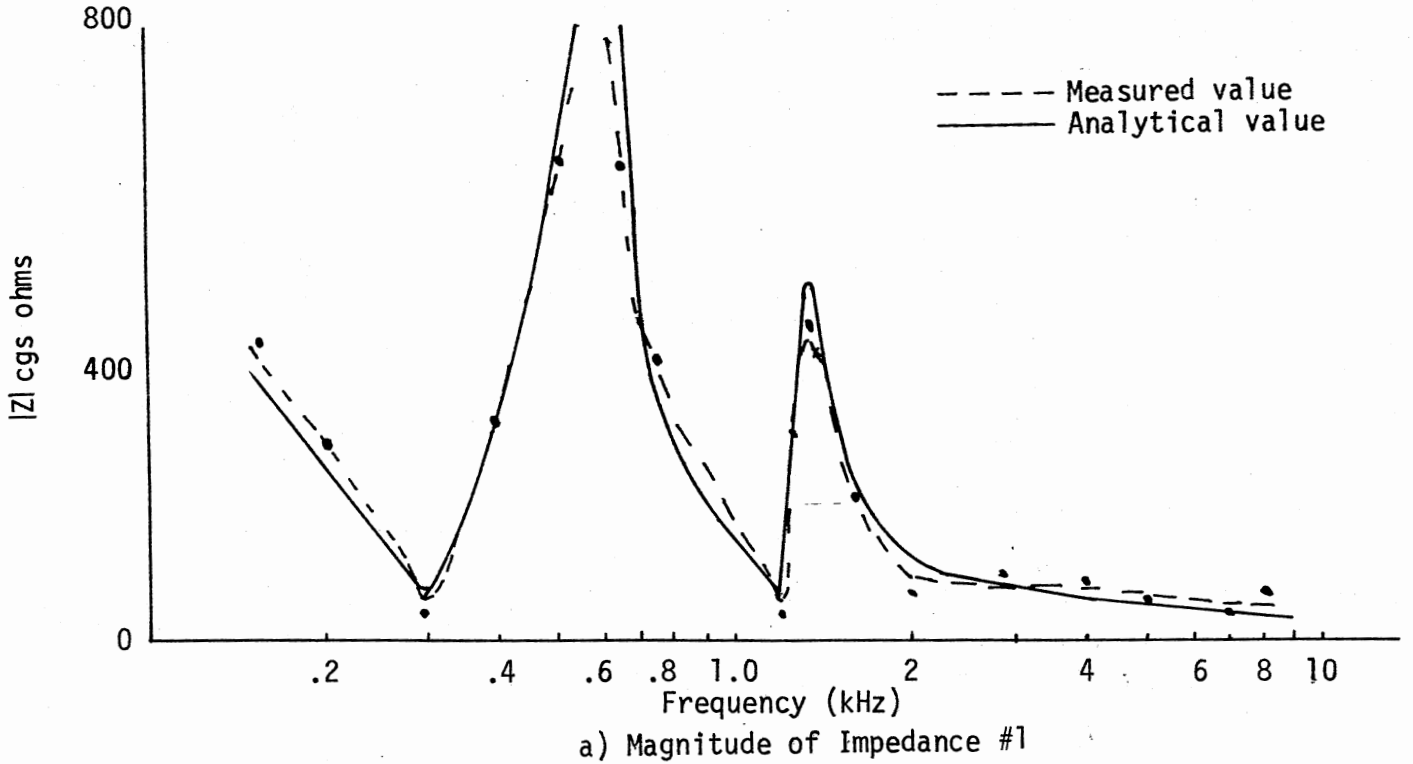

a) Magnitude of Impedance #1

Figure 27. Measured and Analytical Values of Standard Impedance Shown in Figure 24

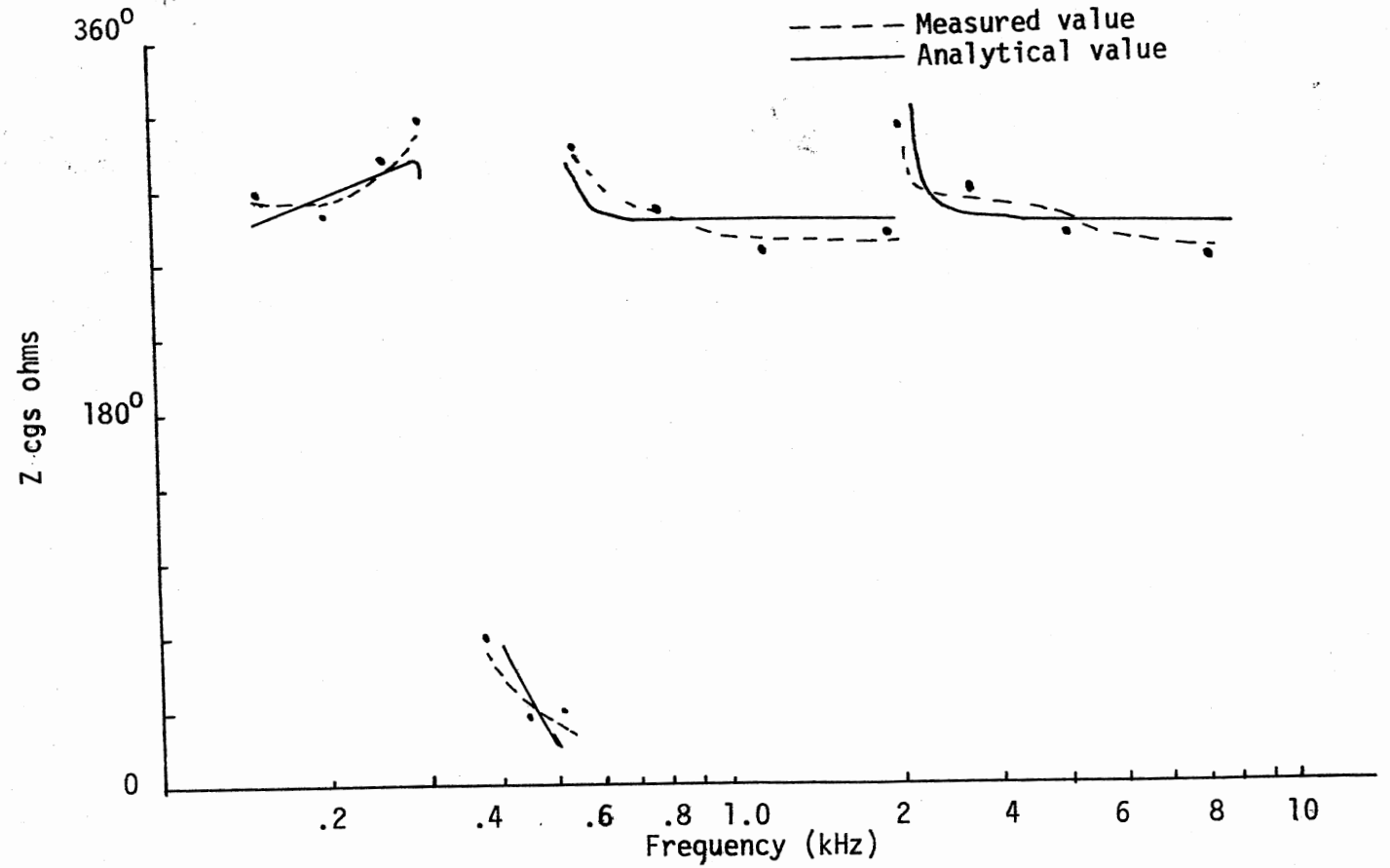

b) Phase of Impedance #1

Figure 27 (continued)

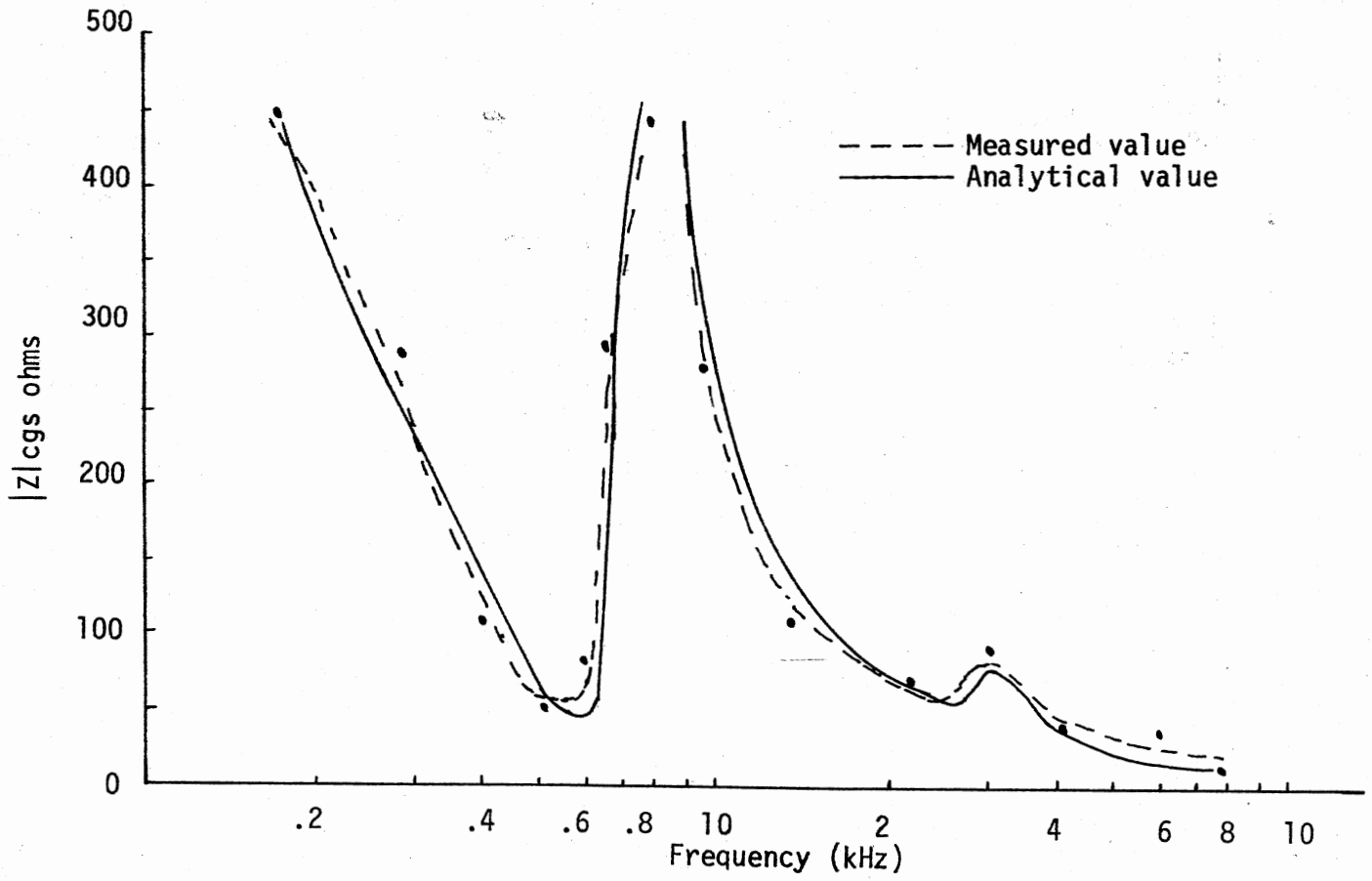

c) Magnitude of Impedance #2

Figure 27 (continued)

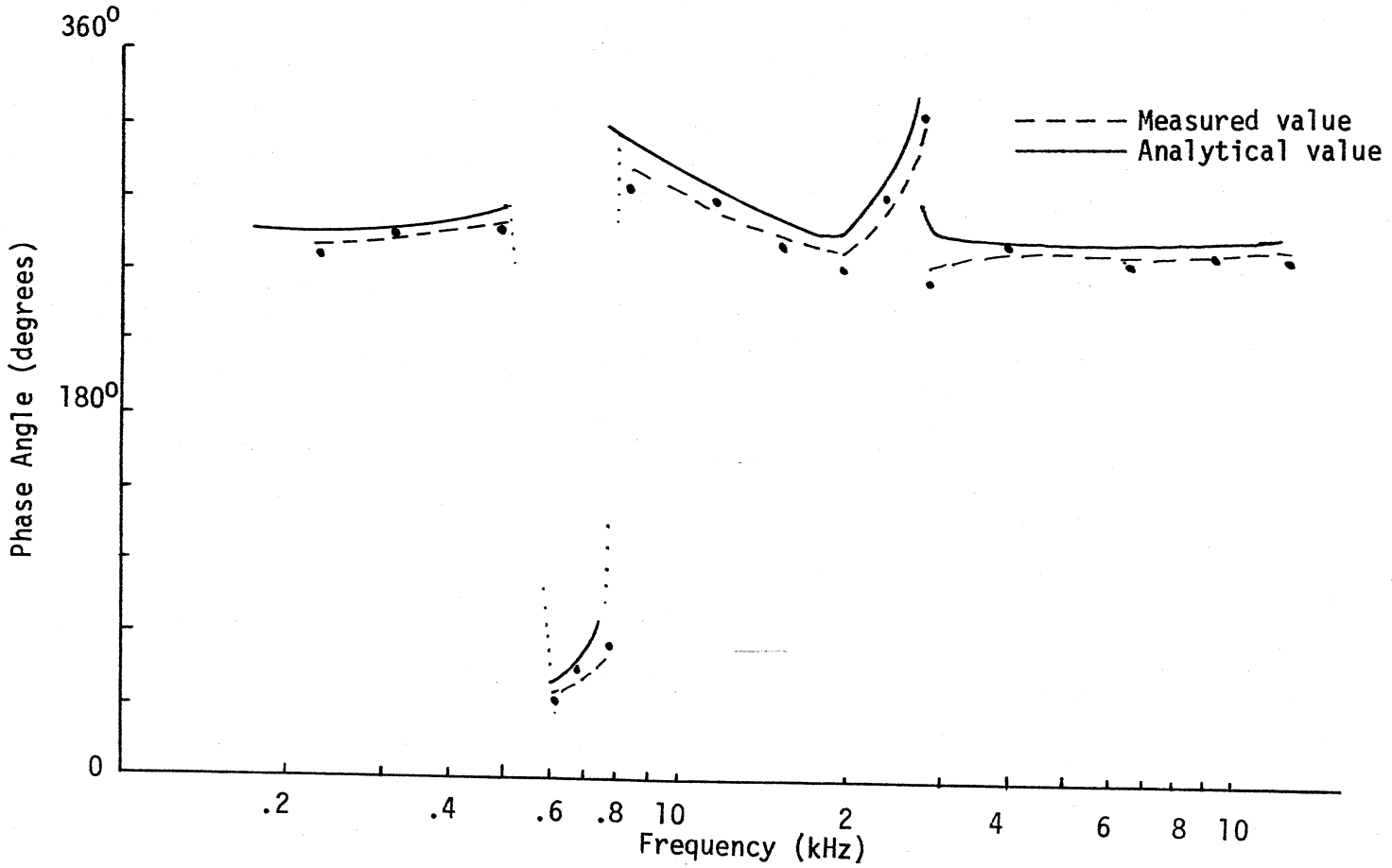

d) Phase of Impedance #2

Figure 27 (continued)

elements of the instrument. The mathematical model is very sensitive to the errors in measurement of dimensions, particularly at high frequencies. In the low frequency region, the accuracy of impedance measurement obtained by using this technique is of the same order of magnitude as that obtained by using a constant volume velocity technique described in the following section.

3.4 Validation of Constant Volume Velocity Assumption

Most of the methods used for measurement of acoustic impedance of the human ear are based on the assumption that volume velocity of the sound source is constant. If the volume velocity of the source is known, then the measured sound pressure is proportional to the acoustic impedance of the medium or the enclosure where the pressure is developed. Figure 28 shows the schematic diagram of the instrumentation required for impedance measurement using this technique. A constant volume velocity source is realized by placing a high resistance tube (a narrow tube) between the sound source and the impedance to be measured. Pressure at the impedance is measured by a probe tube. To minimize the loss of volume velocity through the probe, a high resistance tube is also introduced between the probe and the microphone.

To measure the unknown impedance, first a known impedance, Z_K, is connected to the device, and pressure P_K is measured. The measured pressure is related to the impedance by the following equation:

$$P_K = Z_K * U \tag{3.12}$$

where U is the volume velocity assumed to be constant.

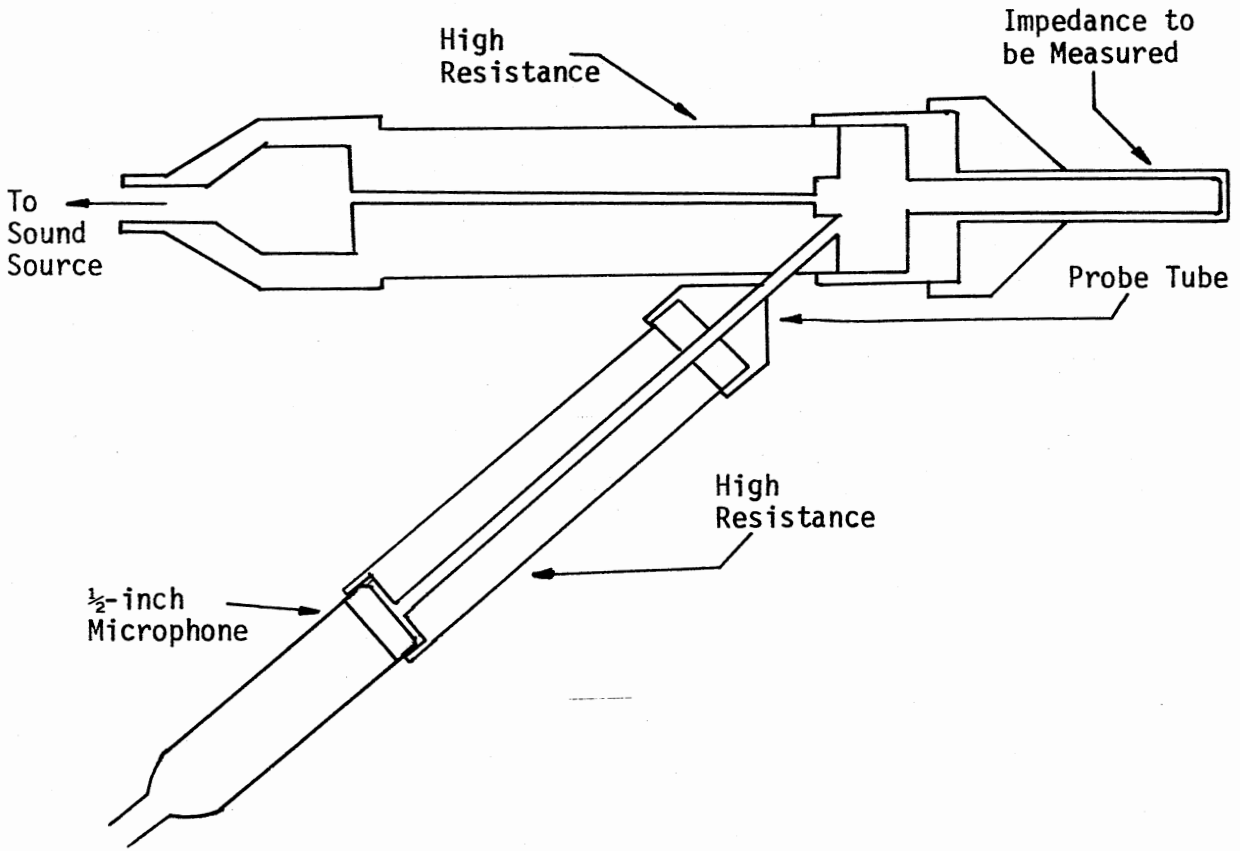

Figure 28. Instrumentation for Impedance Measurement Using Constant Volume Velocity Assumption

A smilar equation can be written for the pressure P_U that exists when the unknown impedance is connected to the instrument.

$$P_U = Z_U * U \tag{3.13}$$

Dividing Equation (3.12) by Equation (3.13), and solving for Z_U, the result is

$$Z_U = (P_U/P_K)/Z_K \tag{3.14}$$

Since the output voltage of the microphone is directly proportional to the input pressure, Equation (3.14) can be written as

$$Z_U = (V_U/V_K) * Z_K \tag{3.15}$$

where V_U and V_K are the microphone voltages with Z_U and Z_K connected to the instrument, respectively. Thus, the unknown impedance is obtained in terms of the known impedance. The advantage of the method is that it is very simple, and no complex modeling of the acoustic elements of the device is required. It does, however, require the mathematical modeling of the known impedance. The accuracy of the measured impedance, therefore, depends on the accuracy of the mathematical model.

To check the validity of the constant volume velocity assumption and to compare the accuracy of impedance measurements using this technique with that obtained by using the two-pressure measurement technique described in this dissertation, the following experiment was designed.

Two acoustic resistors were made by boring a 2-mm diameter hole in a cylinder 6 cm long. The resistance of this tube is quite large compared to the impedance that will be used as the unknown impedance in

the experiment described below. A tube blocked one end, as shown in Figure 24(a) is used as a standard impedance, and the tube shown in Figure 24(b) is used as the unknown impedance. With the standard impedance connected to the device, output voltage of the microphone and its phase with respect to source voltage is measured at each frequency in the range of 100 Hz to 1000 Hz. The same measurements were taken with the unknown impedance connected to the device. The magnitude and phase of the unknown impedance is then calculated using Equation (3.15). The measured quantities are plotted as a function of frequency as shown in Figure 29. It is observed that the measurements can be made within ten percent error with the method, but the measurements cannot be continued at higher frequencies because of the attenuation in the probe tube.

The main advantage of the instrument described in this dissertation over the constant volume velocity technique is its wide operating frequency range. This instrument is employed to measure acoustic impedance of a human ear. The measurement procedure and the results of the measurements are presented in the next chapter.

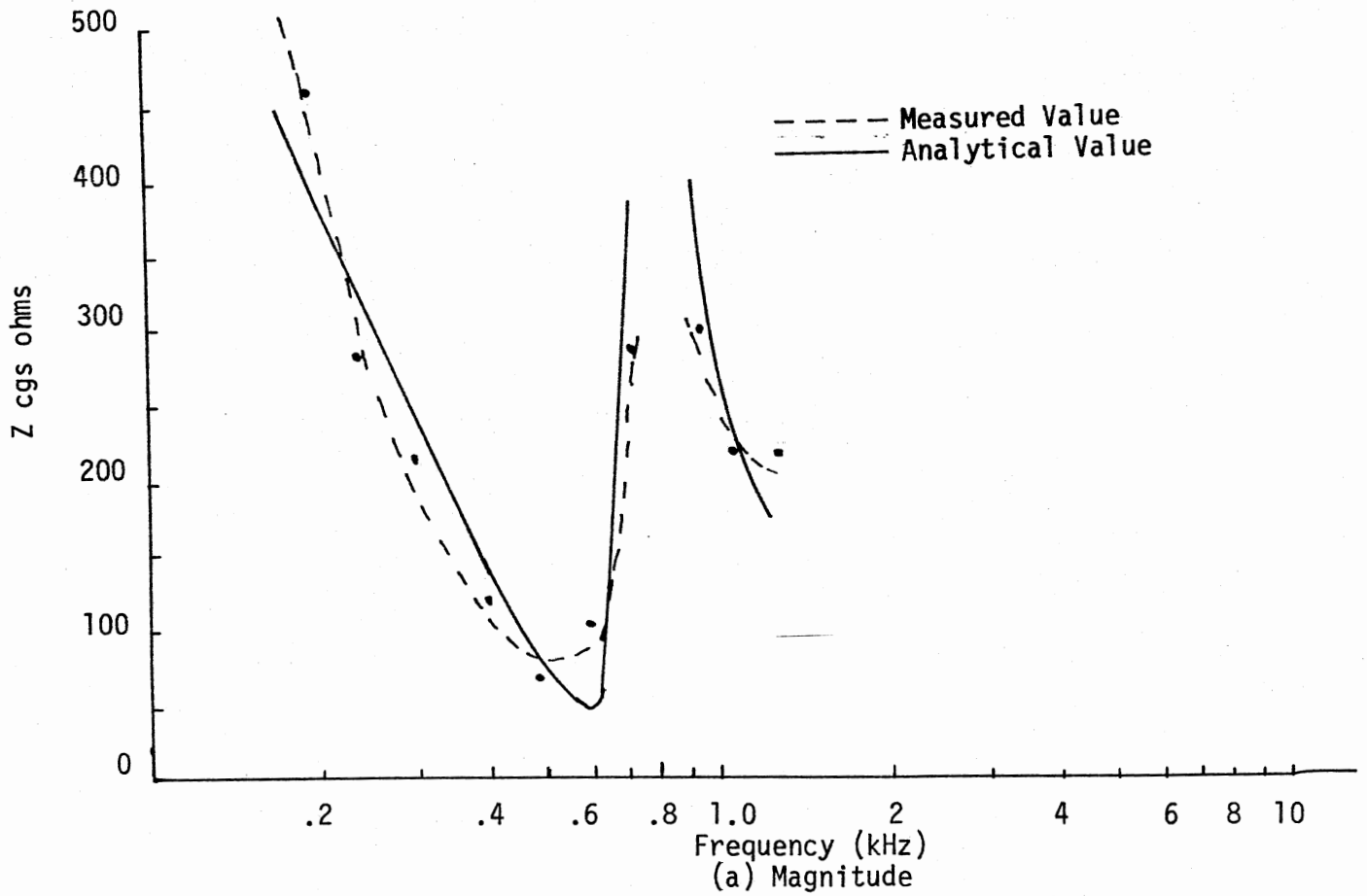

Figure 29. Impedance Measurement Using Constant Volume Velocity Assumption

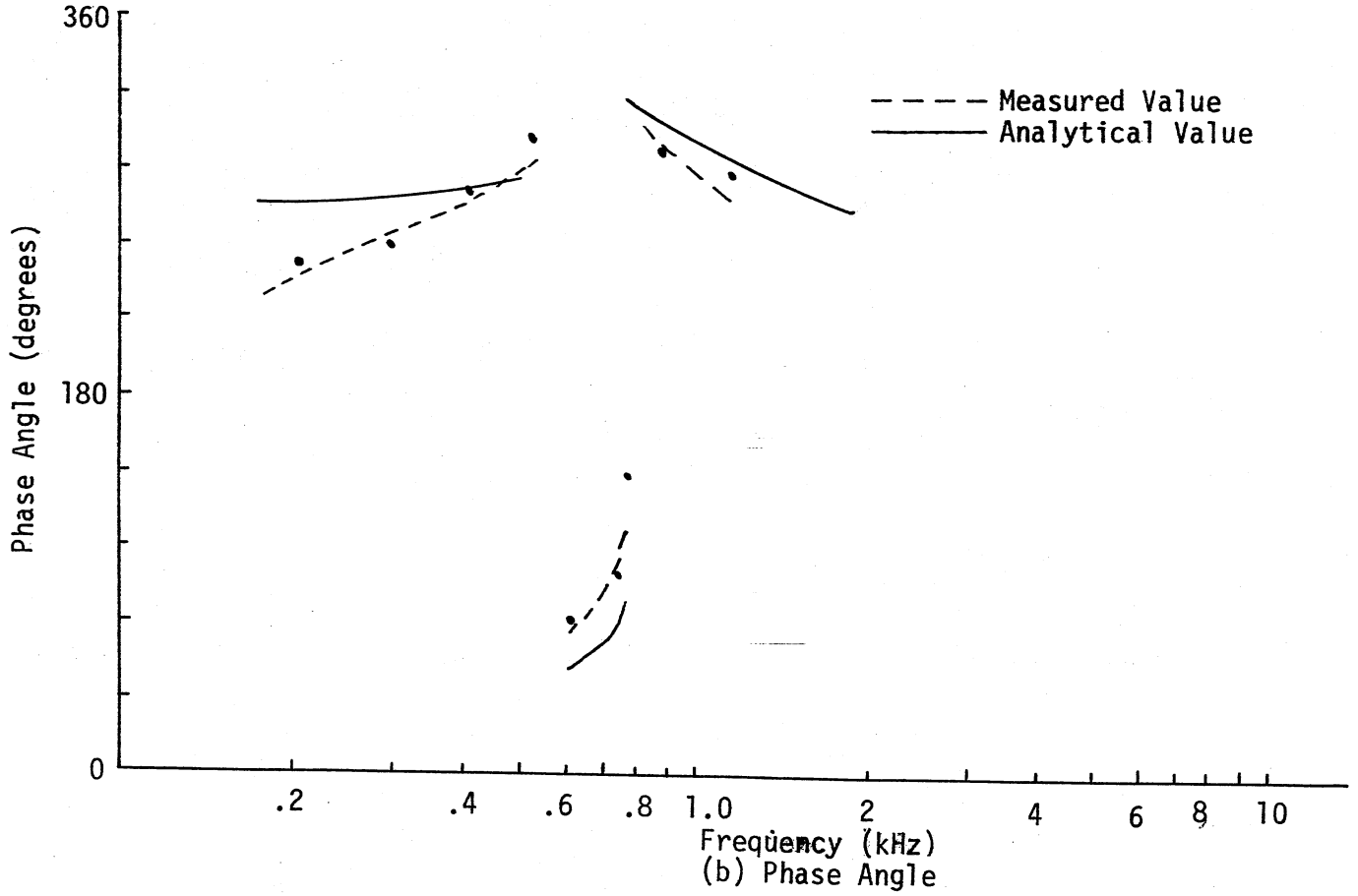

(b) Phase Angle

Figure 29 (continued)

CHAPTER IV

EAR IMPEDANCE MEASUREMENT

4.1 Introduction

The instrument to measure the acoustic impedance based on the two-pressure measurement principle was described in the last chapter. The next objective of the present study is to measure the acoustic impedance of a human ear. This chapter contains a discussion of the impedance measurements taken on a human ear.

4.2 Measurement Procedure

A major problem encountered in ear impedance measurement is in achieving an acoustic seal between the measuring instrument and the ear canal. In the present investigation, the instrument is mounted on a headset in order to minimize any relative motion between the instrument and the subject's head. A pair of ear protectors is used for this purpose. A special fixture is made on one cup of the ear protector as shown in Figure 30. The impedance tube of the instrument passes through the ball and socket joint mounted on the protector. This allows rotational and translational motion of the instrument relative to the ear, thus allowing the impedance tube to be inserted in the ear canal at a proper angle and can be locked in the proper position. An ear plug made of a soft material is fixed on the tip of the impedance tube. When

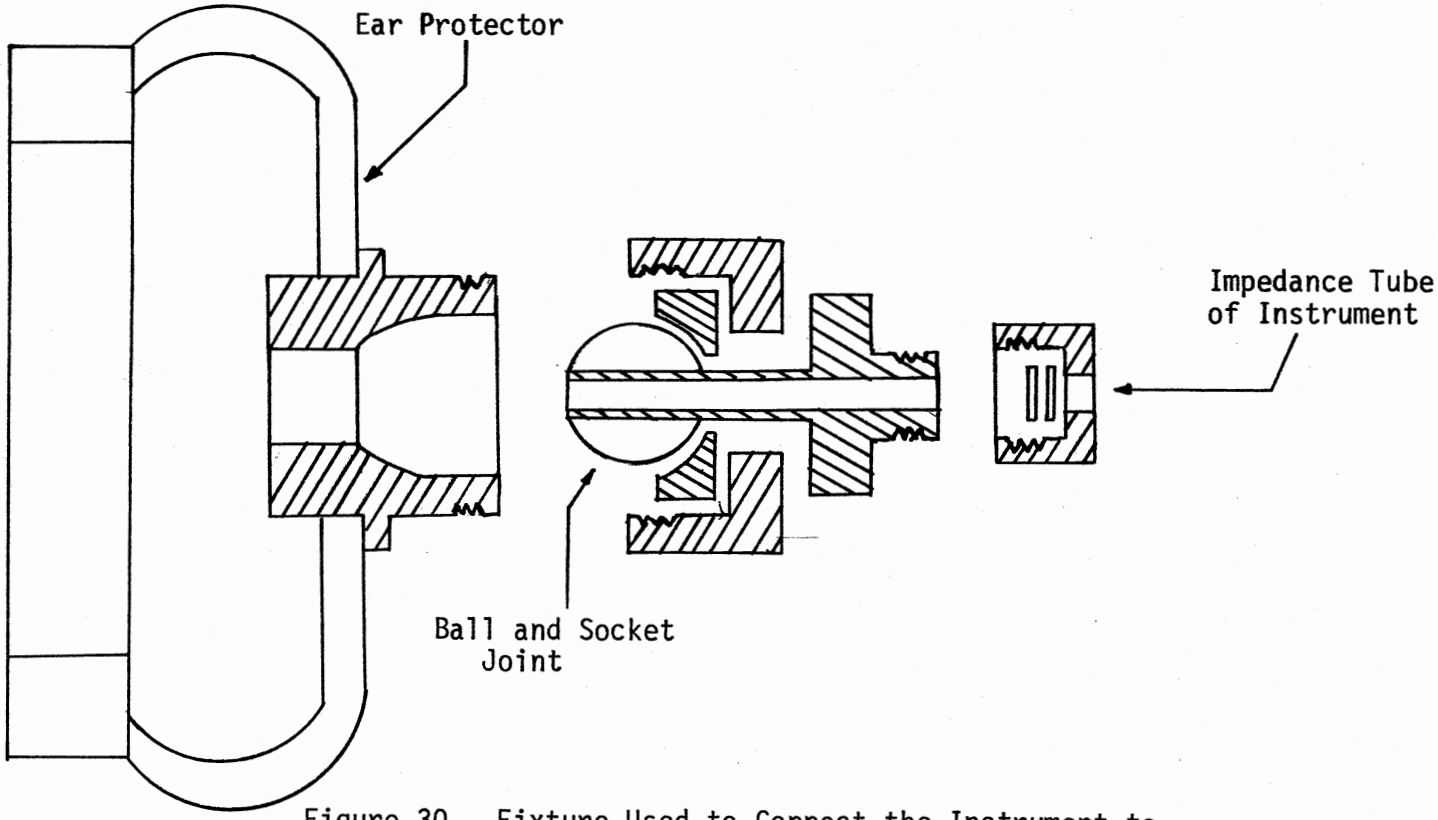

Figure 30. Fixture Used to Connect the Instrument to the Ear Canal

inserted inthe ear canal, the ear plug assumes the profile of the ear canal and acts as a perfect seal.

The instrument is connected to a sound source through a flexible tube and a conical shaped cover as shown in Figure 31. Gaps between the speaker and the cover are sealed by sealing material so that when the instrument is connected to the sound source and the ear canal, the whole unit is leak-proof.

To check for leaks, a manometer made of plastic tubing is connected to the conical cover through a narrow tube. With the instrument connected to the ear canal, the pressure in the ear is increased by using a syringe, as shown in Figure 31. The pressure is monitored on the manometer. The difference in liquid level of the manometer was maintained for a period of time indicating the absence of leaks in the connections.

It was mentioned in the last chapter that during the impedance measurement, the pressure level in the ear canal should be maintained below 80 db. This was achieved by monitoring the output voltages of both microphones. At any frequency, pressure in the instrument was adjusted so that the voltages of the microphones fell below the curves shown in Figure 32.

The curves shown in Figure 32 represent the output voltages of the microphones when the probes are subjected to 80 db pressure. These curves are obtained by simulating the probes on a digital computer.

The block diagram of the simulated system is shown in Figure 33, where the probe is represented by its four-pole network model. S is the sensitivity of the microphone, and G(jw) is the gain of the high pass R-C filter.

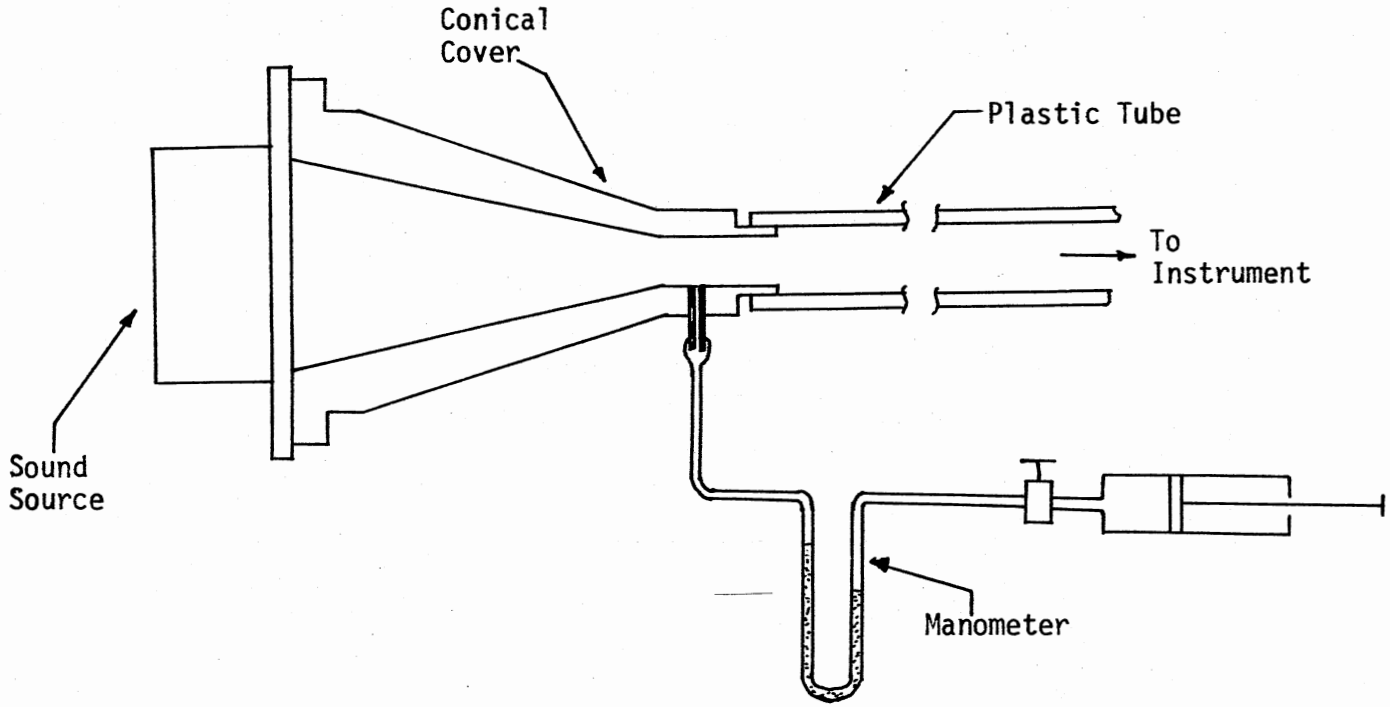

Figure 31. Sound Source Connections and Scheme to Check Leaks

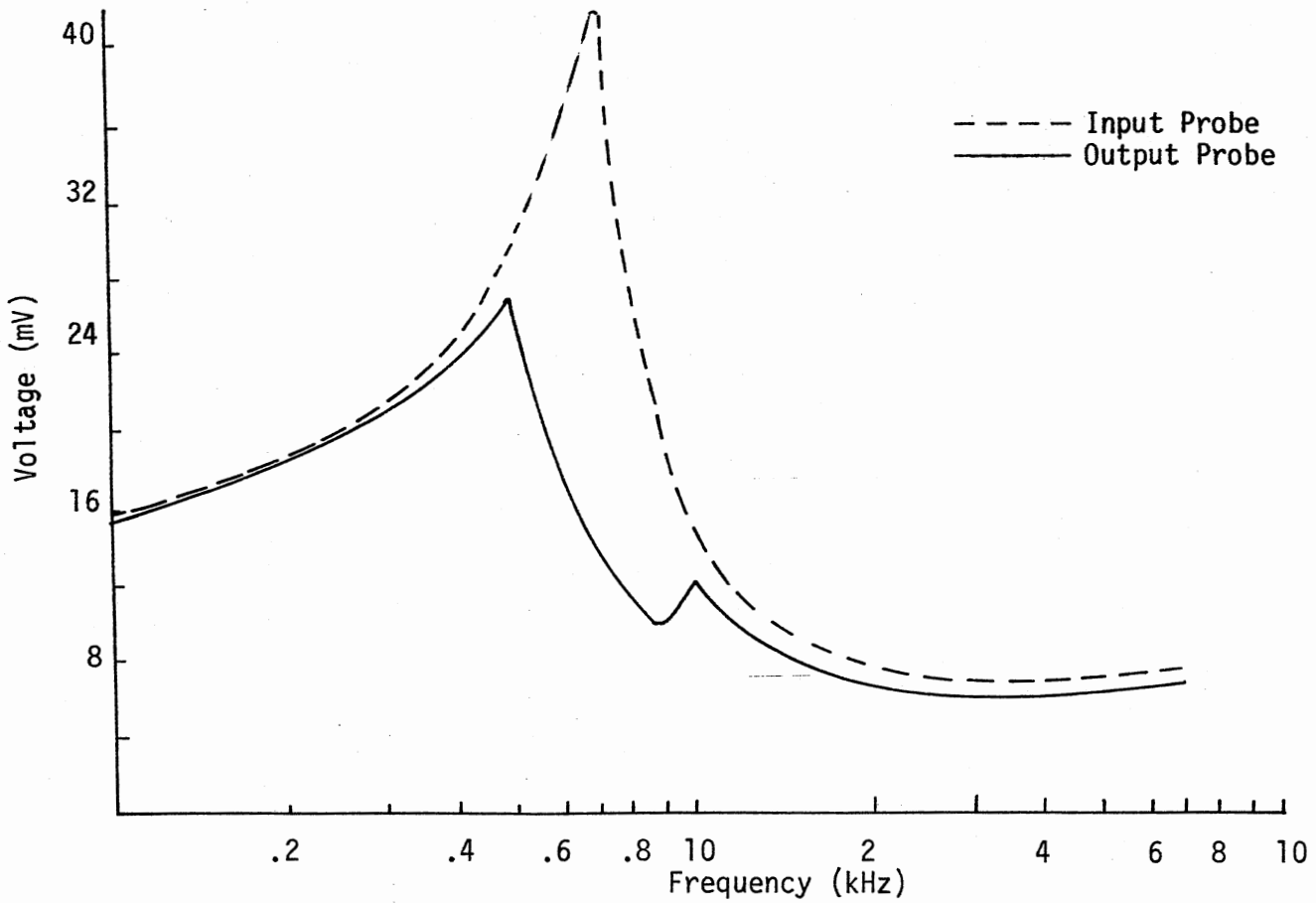

Figure 32. Output Voltages of Simulated Probes for Input Pressure of 80 db

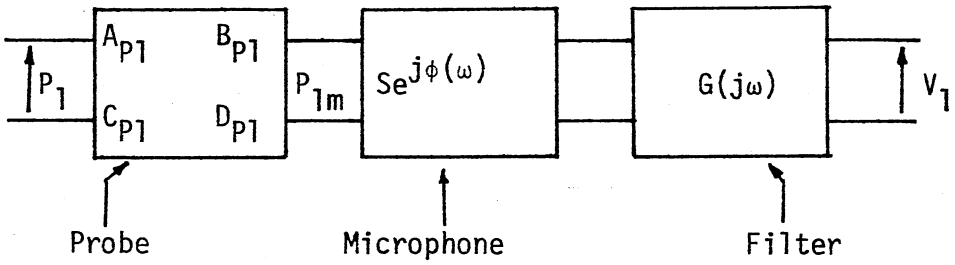

Figure 33. Block Diagram of the Simulated Probe Tube

The pressure input to the probe tube is related to the measured voltage by the following equations

$$P_1 = (A_{P1} + B_{P1}/Z_{mic})* P_{1m} \tag{2.31}$$

$$V_1 = S * G(j\omega) * P_{1m} \tag{3.16}$$

hence

$$V_1 = S * G(j\omega) * P_1/(A_{P1} + B_{P1}/Z_{mic}) \tag{3.17}$$

Employing Equation (3.17), V_1 is calculated for the frequency range of 100 Hz to 7 kHz with P_2 kept at 80 db. The graph of V_1 versus frequency is shown in Figure 32.

The complete experimental setup for ear impedance measurement is the same as shown in Figure 26. The measurements were carried out over the frequency range of 150 Hz to 7 kHz in steps of 50 Hz or 100 Hz. At each frequency, output voltages of both microphones and phase angle between them were recorded. From these data, impedance of the ear was calculated using equations derived in Chapter III. The calculated impedance and the resulting impedance profile are presented in the next section.

4.3 The Impedance Profile

Employing the equations of section 3.2.4, the load impedance of the ear is calculated from the voltage and phase angle recorded during the experiment described in the last section. The calculated quantity represents the impedance at the entrance to the ear canal where the end of the instrument probe is placed. To obtain the impedance of the

ear drum, the effect of the ear canal must be taken into account.

In the previous studies, the ear canal has been represented as a pure compliance--the assumption that is justified only at low frequencies. At high frequency, resistive and inertia effects must be taken into account in modeling the ear canal.

In the present investigation, the ear canal is represented by a transmission line model. A four-pole network analog of the canal is shown in Figure 34, where Z_e represents the impedance of the ear drum to be measured, and A, B, C, and D are the four-pole parameters defined by Equation (2.17). Z_C and τ appearing in Equation (2.17) are the propagation constant and the characteristic impedance of the ear canal, respectively.

The calculated impedance, Z_U, is related to Z_e by the following equations.

$$Z_U = \frac{AZ_e + B}{CZ_e + D} \tag{3.19}$$

The above equation requires knowledge of the dimensions of the ear canal. To measure them, the ear canal was filled with a known volume of liquid. The diameter of the canal was obtained by measuring the dimensions of the impression on the ear plug. From the two measurements, the length of the canal was approximated assuming a right circular cylindrical shape. The impedance of the ear drum was then calculated using Equation (3.19). A plot of the real and imaginary parts of the impedance is shown in Figure 35 up to 7 kHz. This is the static impedance profile of a human ear. On the same graph, a region enclosed by dotted lines is shown representing the range of

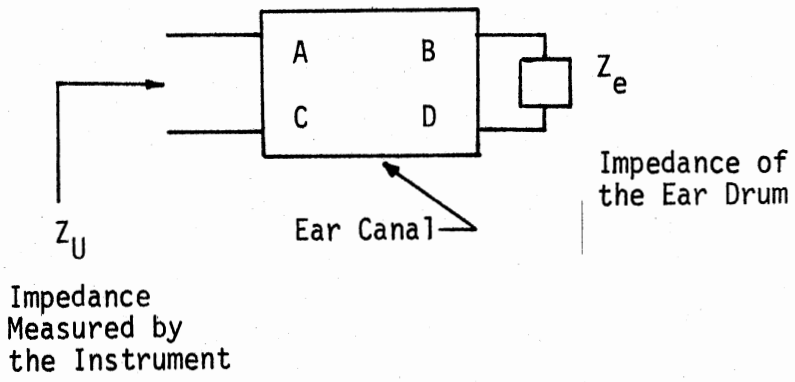

Figure 34. Four-pole Network Analog of the Ear Canal

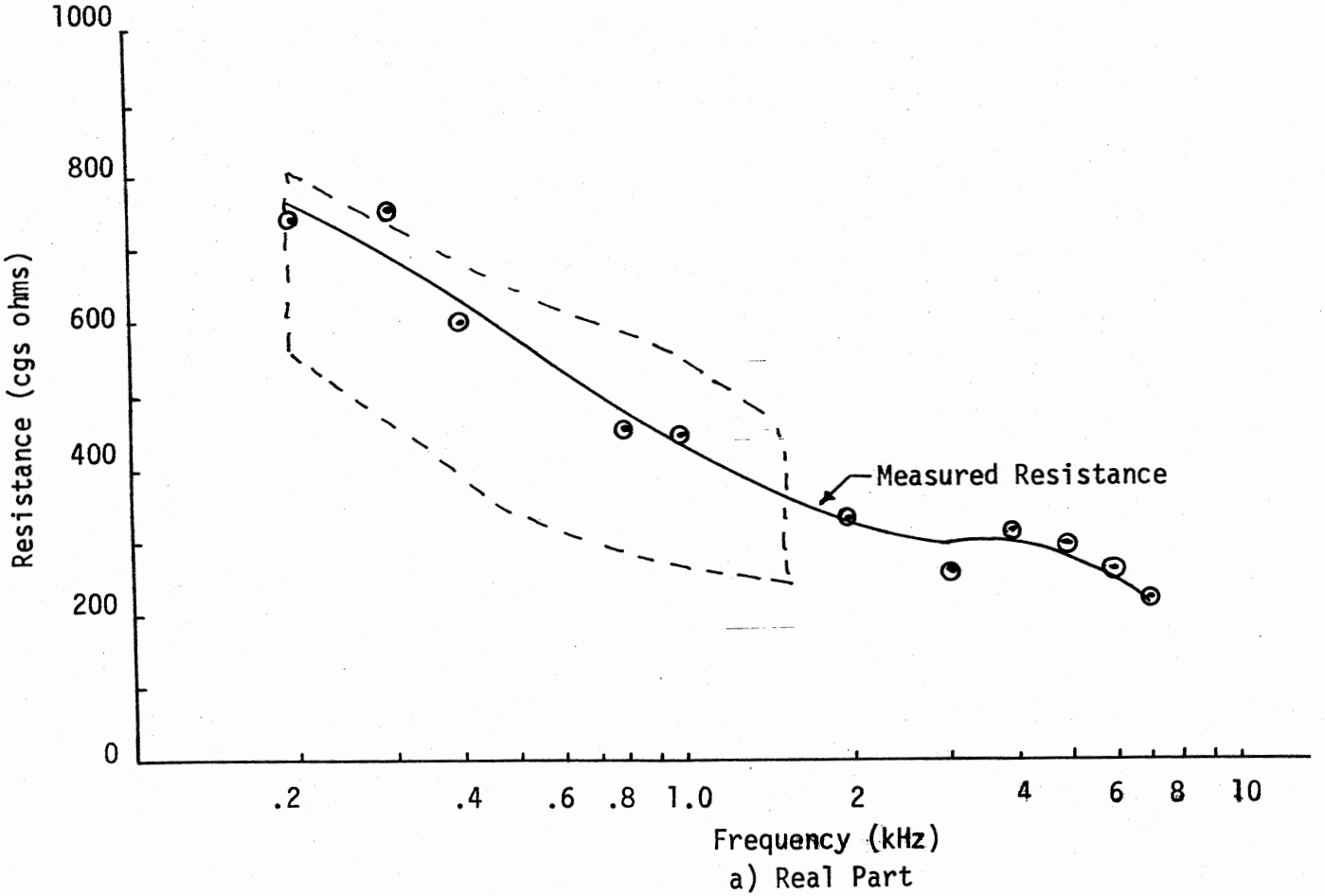

Figure 35. Impedance Profile of a Human Ear

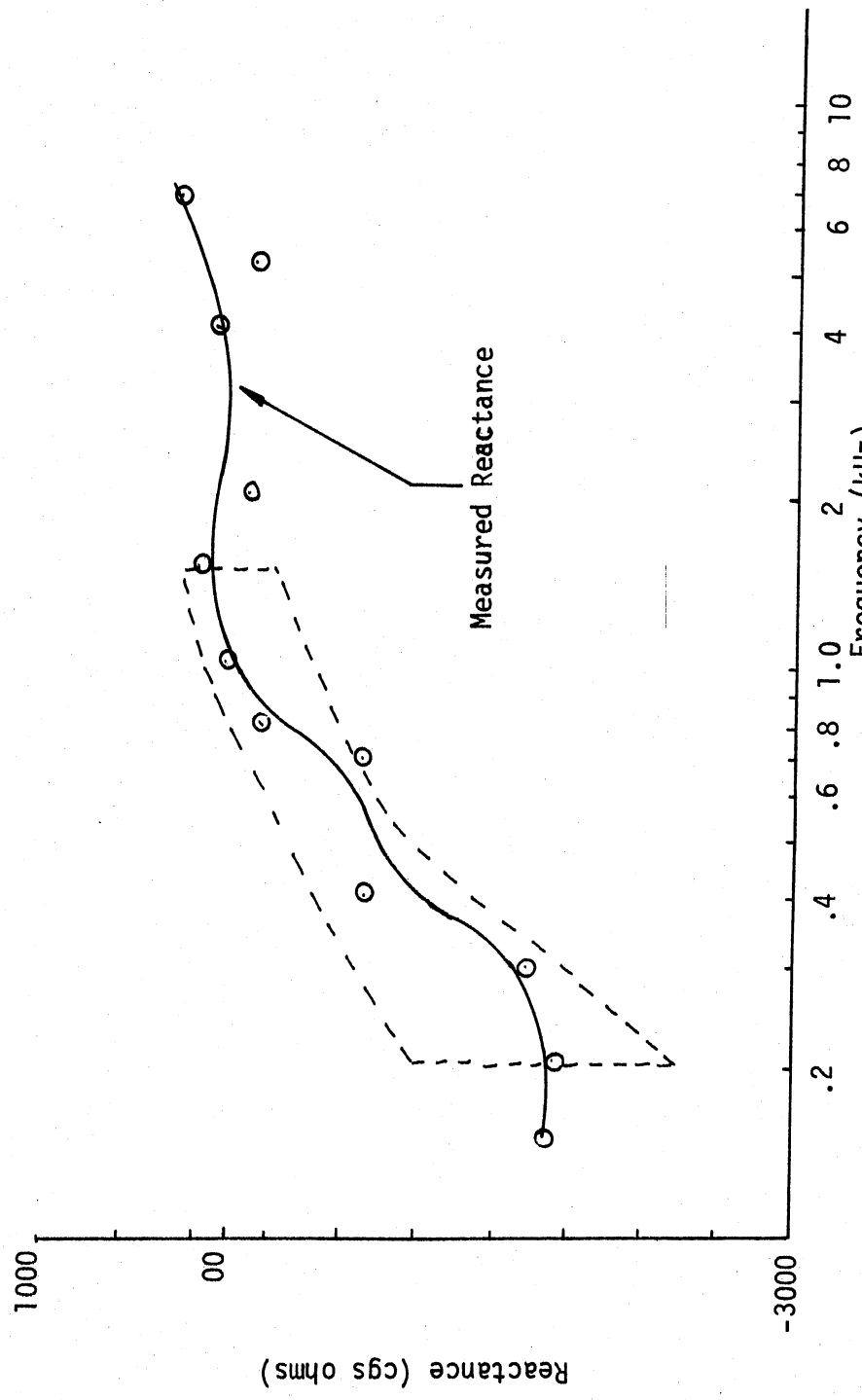

b) Imaginary Part

Figure 35 (continued)

values associated with the acoustic impedance of a normal human ear. This region was obtained from impedance measurements reported by other investigators. The impedance profile found in the present investigation falls in this region.

The impedance measurements reported here are taken up to 7 kHz. The measurements above 7 kHz were not taken for two reasons. First, at high frequencies, the attenuation in the probe tubes makes the pressure measurement difficult. Second, the mathematical model is extremely sensitive to errors made in tube dimensions measurement at high frequency. Since it is not possible to measure the dimensions of the ear canal with the accuracy required by the mathematical model, high frequency impedance measurement seems inappropriate.

CHAPTER V

CONCLUSIONS AND RECOMMENDATIONS

The main objective of the dissertation was to develop an instrument to measure the acoustic impedance of a human ear over a wide frequency range. The need for such an instrument was demonstrated by the results of other studies of ear impedance which indicated that (1) the ear has several natural frequencies above 2 kHz, and (2) that impedance profiles may have potential for diagnostic purposes especially if impedance could be measured in the 2 kHz to 10 kHz range. This objective has been achieved. The instrument reported in the dissertation measures impedance up to 7 kHz with the error in measurement less than 12 percent in magnitude and phase. This instrument was employed to measure acoustic impedance of a human ear. The ear impedance measurement served a dual purpose. First, the impedance profile up to 7 kHz was obtained, and second, the measurement procedure revealed the difficulties encountered in taking impedance measurements.

A difficulty in acoustic impedance stems from the fact that volume velocity, which could be conveniently used to determine an acoustic impedance, cannot be measured directly. In the measurement technique described in the dissertation, volume velocity is obtained indirectly by measuring pressures at two points on a tube of known impedance. This tube is connected to the unknown impedance, and impedance calculations can be made without having to calculate volume velocity directly.

The accuracy and operating frequency range of the instrument based on this technique depends on the accuracy of the equations which define the tube impedance and the frequency range over which the equations are valid.

In the present investigation, equations for evaluating tube parameters were obtained from the distributed parameter theory of fluid transmission lines. The validity of these equations was checked by performing an experiment on a short tube. In the experiment, the tube was subjected to sound waves, and the pressures existing at the input and output ends of the tube were measured. The measured pressure ratio was then compared with the analytically calculated pressure ratio. The experimental and analytical pressure ratios were in good agreement (less than five percent error) except near the resonant frequency of the tube, indicating that equations used in modeling the tube were accurate except at the resonance frequencies. While calculating the analytical pressure ratio, end correction was applied to find the equivalent length of the tube. The mathematical model of the tube was found to be very sensitive to errors in the measurement of the tube dimensions.

An instrument based on the two-pressure measurement technique was designed. The design of the instrument was influenced greatly by two constraints which had to be satisfied in order to measure the acoustic impedance of a human ear. First, the sound pressure level in the ear canal must be maintained below 80 db so as not to elicit the middle ear muscle reflexes. Second, the instrument must be small to facilitate easy mounting on the headset. The first constraint required the pressure measurement system to be sensitive to pressures below 80 db.

The pressure measurement scheme devised for the instrument used probe tubes with ½-inch microphones connected to two cavities at each end of the impedance tube at the points where pressures were to be measured.

The probe tubes used for pressure measurements caused two problems. The first problem was to relate the pressure measured by the microphone at the exit end of the probe tube to the pressure at the entrance to the probe tube. This was accomplished by employing the mathematical model of the tube. As mentioned earlier in connection with the probe tube experiment, near the resonant frequency of the probe, the experimentally observed pressure ratio was significantly different from the analytically calculated pressure ratio. This required the use of a probe tube of a different length over the frequency range near the resonant frequency of the first probe. For the instrument described in the dissertation, two tubes of different lengths were used as input probes which measured the pressure in the impedance tube. The second problem which played a major role in the design of the instrument was created by the finite input impedance of the output probe tube. The finite input impedance of the output probe tube causes the loss of volume velocity which complicates the calculations of the unknown impedance. To minimize this loading effect, the output probe was desgined so that the input impedance of the probe tube was higher than the impedance of the instrument probe tube at that point. This was achieved by selecting four probes of different lengths and choosing the dimensions of the cavity wherein the probe was introduced. Each probe was used over the frequency range over which its input impedance was higher than that of the other three probes.

The accuracy of the impedance measurement was checked by taking measurements on standard acoustic impedances. It was found that a known test impedance could be measured with an error of less than 12 percent in magnitude and phase.

The instrument was used to measure the static acoustic impedance of a human ear. A special fixture was constructed to mount the instrument on a headset. The instrument was connected to the ear canal through an ear plug. Acoustic seal was checked by increasing a pressure in the ear canal and observing it on a manometer connected to the instrument. The instrument measures impedance at the end of the probe tube in the ear canal. The impedance at the ear drum was found by modeling the ear canal as a transmission line. The impedance profile of a presumed normal human ear was obtained up to 7 kHz. This impedance profile fell within the range for a normal human ear as established in the literature up to 2 kHz. Measurements above 7 kHz were not taken for two reasons. First, above 7 kHz, the attenuation in the probe tubes makes the pressure measurements difficult, and second, at high frequencies the mathematical model of the tube is extremely sensitive to errors in tube dimensions. Inaccuracies in measurement of the ear canal dimensions would introduce significant errors into the ear drum impedance calculations.

The objective of designing the instrument to measure accurately the acoustic impedance of a human ear over a broad frequency range has been achieved, and the impedance profile of a normal ear has been obtained. Although the ability of the instrument to measure acoustic impedance over a wide frequency range makes it a valuagle diagnostic tool, in the present form it is rather inconvenient to use for the routine clinical examinations, particularly because of the requirement

of using different probe tubes during measurement. This limitation can be removed by redesigning the instrument so that a single probe of smaller length (and hence higher resonant frequency) can be employed over a wide frequency range. The instrument in the present form, however, remains as a valuable research tool. Since the primary field of application of this instrument is audiology, future work related to study of the impedance profile as a diagnostic criterion should be undertaken. This work would include taking measurements on several ears with different pathological conditions, and establishing a definite relationship between the impedance profile and the pathological condition of a human ear.

SELECTED BIBLIOGRAPHY

1. Webster, A. G. "Acoustical Impedance, and the Theory of Horns and of the Phonograph." Proc. Natl. Acad. of Sci., Vol. 5, 1919, pp. 275-282.

2. Metz, O. "The Acoustic Impedance Measured on Normal and Pathological Ears." Acta Oto-Larnygologica Supplementum, Vol. 63, 1946, pp. 1-246.

3. Whaley, P. W. "An Acoustic Impedance Meter and Its Value as a Diagnostic Tool." Ph.D. dissertation, Oklahoma State University, 1975.

4. Beranek, L. L. "Acoustical Measurements." New York: Wiley & Sons, 1949.

5. Moller, R. K. "Improved Technique for Detailed Measurement of Middle Ear Impedance." Journal of Acoustical Society of Americal, Vol. 32, No. 2, 1950, pp. 250-257.

6. Zwislocki, J. "Some Measurements of the Impedance of the Ear Drum." Journal of Acoustical Society of America, Vol. 29, No. 3, 1957, pp. 349-356.

7. Pinto, L. H., and Dallos, P. J. "An Acoustic Bridge for Measuring the Static and Dynamic Impedance of the Ear Drum." IEEE Transactions on Bio-medical Engineering, Vol. BME-15, No. 1, 1968, pp. 10-16.

8. Delany, M. E. "The Acoustic Impedance of the Human Ear." Journal of Sound and Vibration, Vol. 1, No. 4, 1964, pp. 455-467.

9. Zwislocki, J. "An Acoustic Method for Clinical Examination of the Ear." Journal of Speech and Hearing Research, Vol. 16, 1963, pp. 303-314.

10. Iberall, A. S. "Attenuation of Oscillatory Pressures in Instrument Lines." Journal of Research of the National Bureau of Standards, Vol. 45, 1950, pp. 85-108.

11. Nichols, N. B. "The Linear Properties of Pneumatic Transmission Lines." ISA Transactions, Vol. 1, No. 1, 1962, pp. 5-14.

12. Rohman, C. P., and Grogan, E. C. "On the Dynamics of Pneumatic Transmission Lines." Transactions of the American Society of Mechanical Engineers, Vol. 79, No. 4, 1957, pp. 853-874.

13. Fay, R. C. "Attenuation of Sound in Tubes." Journal of Acoustical Society of America, Vol. 12, 1940.

14. Doeblin, E. O. "Measurement Systems: Application and Design." New York: McGraw-Hill Book Company, 1966, pp. 401-402.

15. Hilsenrath, J. et al. "Tables of Thermal Properties of Gases." U. S. National Bureau of Standards, Cir. No. 564, Chapters 1 and 2, 1955.

VITA

Tushar Shankar Kale

Candidate for the Degree of

Doctor of Philosophy

Thesis: MEASUREMENT OF ACOUSTIC IMPEDANCE OF THE HUMAN EAR

Major Field: Mechanical Engineering

Biographical:

Personal data: Born in Nagpur, India, February 8, 1952, the son of Mr. and Mrs. S. N. Kale.

Education: Graduated from Dharampeth High School, Nagpur, India, in April 1967; received the Bachelor of Engineering (Electrical) degree from Nagpur University, Nagpur, India, in 1972; received the Master of Engineering (Automation) degree from the Indian Institute of Science, Bangalore, India, in 1974; completed requirements for the Doctor of Philosophy degree at Oklahoma State University in December, 1979.

Professional Experience: Graduate research and teaching assistant, School of Mechanical and Aerospace Engineering, Oklahoma State University, August 1974 to present.